Supplementary Information

Oxygen-Vacancy–Driven Stabilization of Tetragonal ZrO_2

Zi-Zhan He[1], Teng-Fei Li[1], Lin Chen[1], Zhi-Pan Liu[1,2]*, Cheng Shang[1]*

[1]Collaborative Innovation Center of Chemistry for Energy Material, Shanghai Key Laboratory of Molecular Catalysis and Innovative Materials, Key Laboratory of Computational Physical Science, Department of Chemistry, Fudan University, Shanghai 200433, China
[2]Key Laboratory of Synthetic and Self-Assembly Chemistry for Organic Functional Molecules, Shanghai Institute of Organic Chemistry, Chinese Academy of Sciences, Shanghai 200032, China

CONTENT

1. G-MBNN potential architecture 1
2. SSW-NN method for generating G-NN potential 2
3. G-NN potential Training data 3
4. Benchmark of G-NN calculations against DFT 5
5. Per-metal Formation Energy and Gibbs Free Energy of XZrO Systems 11
6. Bader charge analysis of $ZrO_{1.69}$ 12
7. Thermodynamic data for HZrO systems 13
8. Supplementary Figures of the NN potential test and NaZrO System 15
9. Supplementary Figures of the KZrO System 17
10. Supplementary Figures for HZrO and KZrO 18
11. Supplementary Figures of the CaZrO System 18
12. Supplementary Figures for MgZrO system 19
13. Supplementary Figures of HZrO System 20
14. Supplementary Figures of the ZrO_{2-x} System 20
15. The formation energy calculations of XZrO solution 21
17. Synthetic method 25
18. Characterization 25
19. References 25
20. XYZ Coordinates of Key Structures 26

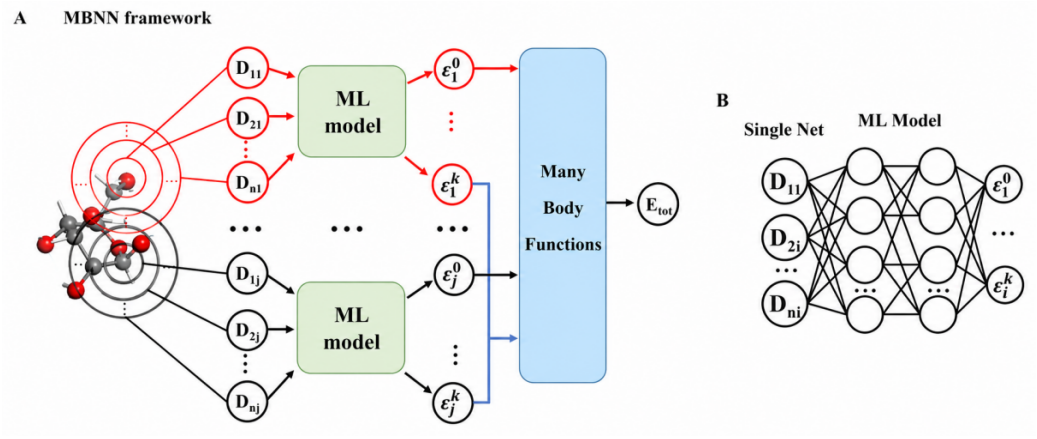

Scheme S1. Architecture of the many-body function corrected neural network potential (MBNN). (A) Each atomic ML model, the feed-forward neural network (NN) utilized in this work as shown in (B), outputs a series of coefficients ε_i^k that acts as the parameters for different many-body functions. The total energy of system is written as the sum of these many-body functions. (B) The implementations of the atomic ML model with the feed-forward NN. Reprinted with permission from Hu, Z.-Y. et al. ACS Catal. 2025, 15, 7015. Copyright 2025 American Chemical Society.

1. G-MBNN potential architecture

In this work, we utilized the many-body function corrected global neural network (MBNN) scheme to construct the global NN (G-NN) potential, as shown in Scheme S1. The input nodes to NN are a set of structural descriptors of a structure, as discussed in our previous works.[1-3] The neural network (NN) architecture is illustrated schematically in Scheme S1. As depicted in Scheme 1A, the input nodes consist of a set of power-type structural descriptors (PTSD),[2] denoted as {Di}, which are derived from the Cartesian coordinates {Ri}. Two examples of PTSDs are provided in Eqs. S3 and S4, while additional examples can be found in Ref. [2].

$$f_c(r_{ij})=\begin{cases}0.5\times\tanh\left(1-\frac{r_{ij}}{r_c}\right), & \text{for } r_{ij}\le r_c\\ 0, & \text{for } r_{ij}>r_c\end{cases} \qquad (S1)$$

$$R^n(r_{ij})=r_{ij}^n\cdot f_c(r_{ij}) \qquad (S2)$$

$$D_i^{\alpha}=\sum_l\left[\sum_m\sum_{j\neq i}R^n(r_{ij})Y_{lm}(\mathbf{r}_{ij})\right]^2 \qquad (S3)$$

$$D_i^{\beta}=\sum_l\left[\sum_m\sum_{j,k\neq i}R^n(r_{ij})\cdot R^m(r_{ik})\cdot R^p(r_{jk})\cdot\left(Y_{lm}(\mathbf{r}_{ij})+Y_{lm}(\mathbf{r}_{ik})\right)\right]^2 \quad (S4)$$

In these Eqs, r_{ij} represents the distance between atom i and j, while θ_{ijk} denotes the angle centered at atom i with atoms j and k as neighbors (where i, j, and k are atom indices). f_c is the cut-off function, which reduces to zero beyond the cut-off distance r_c. The combination of the power function and the spherical harmonic function (Y_{Lm}), similar to atomic wavefunctions, provides a convenient way to couple the radial and angular information of atoms.As illustrated in Scheme 1B, the feed-forward NN generates a vector that includes the atomic energy ε_i^0 and a series of coefficients ε_i^k (where k=1,2,3,…). These coefficients ε_i^k are employed to construct various many-body functions, such as single-body (f_s), two-body (f_d), and three-body (f_t) functions. Consequently, the total energy E_{tot} can be expressed as the sum of both atomic energies and many-body functions, as shown in Eq. S5, with these many-body functions defined in Eqs. S6–S9:

$$E_{tot}=\sum_{s=1}^{n_s}\sum_{i=1}^{n_a}f_s(\varepsilon_i^s)+\sum_{d=1}^{n_d}\sum_{i=1}^{n_a}\sum_{j\neq i}^{n_a}f_d(\varepsilon_i^d,\varepsilon_j^d,r_{ij})+\sum_{t=1}^{n_t}\sum_{i=1}^{n_a}\sum_{j\neq i}^{n_a}\sum_{k\neq i,j}^{n_a}f_t(\varepsilon_i^t,\varepsilon_j^t,\varepsilon_k^t,r_{ij},r_{ik},r_{jk},\theta_{ijk}) \quad (S5)\cdots$$

$$f_s=\lambda\varepsilon_i^s \quad (S6)$$

$$f_d=\lambda\frac{\varepsilon_i^d\varepsilon_j^d}{r_{ij}^{m_d}}f_c(r_{ij}) \quad (S7)$$

$$f_t=\lambda\frac{\varepsilon_i^t\left(\varepsilon_j^t+\varepsilon_k^t\right)^{l_t/2}+\cos(\theta_{ijk})}{r_{ij}^{m_t}\cdot r_{ik}^{m_t}\cdot r_{jk}^{m_t}}f_c(r_{ij})f_c(r_{ik})f_c(r_{jk}) \quad (S8)$$

$$f_c(r_{ij})=0.5*\left[1-\tanh\left(\alpha\left(r_{ij}-(r_{cut}/3-\beta)\right)\right)\right] \quad (S9)$$

where ε_i^k generated by the NN act as the parameters. The total number of atoms in the system is denoted by n_a. The numbers of single-body, two-body, and three-body functions in the MBNN architecture are represented by n_s, n_d, and n_t, respectively (with s, d, and t as function indices). The variables λ, m_d, m_t and l_t are adjustable parameters of these functions. The cut-off function f_c in all the equations feature a cut-off radius r_{cut} and the adjustable parameters α and β, as defined in Eq. S9. In the MBNN architecture, the atomic force is analytically derived from Eq. S5. The force component F_u acting on atom u is obtained by taking the derivative of the total energy with respect to its coordinate vector $\mathbf{r}_u$. This process is further connected to the derivatives of the atomic coefficients ε_i^k and the pairwise distance r_{iu}.

2. SSW-NN method for generating G-NN potential

The stochastic surface walking (SSW) algorithm[4] has an automated climbing mechanism to

manipulate a structure configuration from a minimum to a high-energy configuration along one random mode direction. The method was initially developed for aperiodic systems, such as molecules and clusters[5], and has been extended to periodic crystals[6].

The SSW method inherits the idea of bias-potential driven constrained-Broyden-dimer (BP-CBD) method for TS location[7]. In one particular SSW step a modified PES, as shown in Eq. S10, is utilized for moving from the current minimum to a high-energy configuration by adding a series of bias Gaussian potentials. The bias potentials are added one by one consecutively along the direction that defines the walking direction.

$$V=V_{real}+\sum_{n=1}^{H} v_n =V_{real}+\sum_{n=1}^{H} w_n \times \exp\left[-\frac{\left((\mathbf{R}-\mathbf{R}_n)\cdot\mathbf{N}_n\right)^2}{2\times ds^2}\right] \quad (S10)$$

In the equation $\mathbf{R}$ is the current coordination vector of the structure and V_{real} represents the unmodified PES; R_n is the nth local minima along the movement trajectory on the modified PES that is created after adding n Gaussian functions. The Gaussian function can be further controlled by its height w and its width ds. Once the maximum number of Gaussian functions (e.g.H=9) is reached, all bias potentials are removed and the local optimization is performed to quench the structure to a new minimum.

SSW-NN method is a machine-learning-potential-based global optimization method, which combines the global neural network (G-NN) potential with the SSW method for fast and accurate global PES exploration, as implemented in LASP code.[3,8] While traditional DFT calculations are computationally demanding for the global optimization of complex systems, the SSW-NN method provides a general solution for PES scanning with both high efficiency and high accuracy.[9] The G-NN potential is trained based on the DFT dataset and delivers a high speed of PES evaluation, approximately four orders of magnitude faster than DFT.[1,2,10]

3. G-NN potential Training data

Table S1. Structural information of the global PES dataset for G-NN (KZrO.pot) potential training

Species	Natm	cluster	layer	bulk	total	Species	Natm	cluster	layer	bulk	total
Zr13	13	0	8	5	13	O10-Zr22	32	0	1	71	72
O2-Zr8	10	0	62	200	262	O11-K2-Zr5	18	0	62	1515	1577
O3-Zr49	52	0	26	9	35	O12-Zr6	18	0	27	0	27
O4	4	0	50	0	50	O12-Zr8	20	0	0	256	256
O4-Zr4	8	0	47	344	391	O12-Zr40	52	0	9	0	9
O4-Zr22	26	0	14	62	76	O13-Zr7	20	0	17	8	25
O4-K8	12	0	50	899	949	O13-K2-Zr6	21	0	60	1631	1691
O5-Zr27	32	0	2	63	65	O14-Zr8	22	0	0	122	122
O6-Zr4	10	0	0	24	24	O15-Zr8	23	0	39	3395	3434
O6-Zr8	14	0	59	283	342	O15-Zr9	24	0	1	186	187
O6-Zr15	21	0	132	0	132	O15-K2-Zr7	24	0	59	5036	5095

O6-Zr18	24	0	16	76	92	O16-Zr8	24	0	8	89	97
O7-K2-Zr3	12	0	142	1254	1396	O17-Zr16	33	0	22	1	23
O8-Zr4	12	0	99	8669	8768	O18-Zr12	30	0	222	7	229
O8-Zr8	16	0	51	235	286	O20-Zr38	58	0	37	2	39
O8-Zr15	23	0	22	87	109	O30-Zr16	46	0	37	10530	10567
O9-K2-Zr4	15	0	85	1308	1393	O31-Zr16	47	0	14	2368	2382
O10-Zr8	18	0	73	294	367	total	--	0	1553	39029	40582

Table S2. Structural information of the global PES dataset for G-NN (CaZrO.pot) potential training

Species	Natm	cluster	layer	bulk	total	Species	Natm	cluster	layer	bulk	total
Zr13	13	0	8	5	13	O13-Zr7	20	0	17	8	25
Ca4	4	0	267	40	307	O14-Zr8	22	0	0	122	122
Ca16	16	0	393	28	421	O14-Ca2-Zr6	22	0	29	159	188
Ca24	24	0	17	1	18	O14-Ca10-Zr2	26	0	9	374	383
Ca30	30	0	34	6	40	O15-Zr8	23	0	39	3395	3434
Ca32	32	0	538	61	599	O15-Zr9	24	0	1	186	187
O2-Zr8	10	0	62	200	262	O16-Zr8	24	0	8	89	97
O2-Ca30	32	0	22	5	27	O16-Ca6-Zr5	27	0	0	3	3
O3-Zr49	52	0	26	9	35	O16-Ca8-Zr4	28	0	11	436	447
O4	4	0	50	0	50	O16-Ca16	32	0	200	371	571
O4-Zr4	8	0	47	344	391	O17-Zr16	33	0	22	1	23
O4-Zr22	26	0	14	62	76	O18-Zr12	30	0	222	7	229
O4-Ca4	8	0	0	416	416	O18-Ca2-Zr8	28	0	5	462	467
O4-Ca28	32	0	17	3	20	O18-Ca6-Zr6	30	0	49	539	588
O5-Zr27	32	0	2	63	65	O20-Zr38	58	0	37	2	39
O6-Zr4	10	0	0	24	24	O23-Ca23	46	0	63	0	63
O6-Zr8	14	0	59	283	342	O24-Ca6-Zr9	39	0	54	1	55
O6-Zr15	21	0	132	0	132	O24-Ca8-Zr8	40	0	157	164	321
O6-Zr18	24	0	16	76	92	O24-Ca24	48	0	211	0	211
O7-Ca5-Zr1	13	0	8	69	77	O26-Ca32	58	0	19	7	26
O8-Zr4	12	0	99	8669	8768	O28-Ca32	60	0	53	6	59
O8-Zr8	16	0	51	235	286	O30-Zr16	46	0	37	10530	10567
O8-Zr15	23	0	22	87	109	O30-Ca30	60	0	20	11	31
O8-Ca2-Zr3	13	0	3	7	10	O30-Ca32	62	0	62	4	66
O8-Ca4-Zr2	14	0	32	83	115	O31-Zr16	47	0	14	2368	2382
O9-Ca3-Zr3	15	0	196	443	639	O32-Ca30	62	0	41	11	52
O10-Zr8	18	0	73	294	367	O32-Ca32	64	0	707	166	873
O10-Zr22	32	0	1	71	72	O40-Ca10-Zr15	65	0	76	0	76
O12-Zr6	18	0	27	0	27	O80-Ca16-Zr32	128	0	39	0	39
O12-Zr8	20	0	0	256	256	O96-Ca32-Zr32	160	0	10	0	10
O12-Zr40	52	0	9	0	9	total	--	0	4437	31262	35699

Table S3. Structural information of the global PES dataset for G-NN (NaZrO.pot) potential training

Species	Natm	cluster	layer	bulk	total	Species	Natm	cluster	layer	bulk	total

Zr13	13	0	8	5	13	O10-Zr22	32	0	1	71	72
O2-Zr8	10	0	62	200	262	O11-Na2-Zr5	18	0	62	1514	1576
O3-Zr49	52	0	26	9	35	O12-Zr6	18	0	27	0	27
O4	4	0	50	0	50	O12-Zr8	20	0	0	256	256
O4-Zr4	8	0	47	344	391	O12-Zr40	52	0	9	0	9
O4-Zr22	26	0	14	62	76	O13-Zr7	20	0	17	8	25
O4-Na8	12	0	64	1219	1283	O13-Na2-Zr6	21	0	60	1625	1685
O5-Zr27	32	0	2	63	65	O14-Zr8	22	0	0	122	122
O6-Zr4	10	0	0	24	24	O15-Zr8	23	0	39	3395	3434
O6-Zr8	14	0	59	283	342	O15-Zr9	24	0	1	186	187
O6-Zr15	21	0	132	0	132	O15-Na2-Zr7	24	0	58	5204	5262
O6-Zr18	24	0	16	76	92	O16-Zr8	24	0	8	89	97
O7-Na2-Zr3	12	0	141	1254	1395	O17-Zr16	33	0	22	1	23
O8-Zr4	12	0	99	8669	8768	O18-Zr12	30	0	222	7	229
O8-Zr8	16	0	51	235	286	O20-Zr38	58	0	37	2	39
O8-Zr15	23	0	22	87	109	O30-Zr16	46	0	37	10530	10567
O9-Na2-Zr4	15	0	85	1310	1395	O31-Zr16	47	0	14	2368	2382
O10-Zr8	18	0	73	294	367	total	--	0	1565	39512	41077

4. Benchmark of G-NN calculations against DFT

Table S4a. Benchmark of NN+D3 against DFT+D3 energies for CaZrO structures. The energy of the global minimum of each potential function is set to be zero.

Name	DFT+D3	NN+D3	Natom	Err(meV/atom)
Ca10Zr4	0.00	0.00	32	0.00
Ca10Zr4	0.71	0.72	32	0.40
Ca10Zr4	0.39	0.38	32	0.30
Ca10Zr4	0.82	0.77	32	1.49
Ca12Zr4	0.00	0.00	36	0.00
Ca12Zr4	0.24	0.20	36	1.20
Ca12Zr4	0.65	0.64	36	0.35
Ca12Zr4	0.59	0.63	36	1.01
Ca14Zr4	0.00	0.00	40	0.00
Ca14Zr4	0.50	0.56	40	1.49
Ca14Zr4	1.11	1.25	40	3.49
Ca14Zr4	1.12	1.23	40	2.81
Ca16Zr4	0.00	0.00	44	0.00
Ca16Zr4	1.03	0.79	44	5.44
Ca16Zr4	0.12	0.12	44	0.12
Ca16Zr4	0.90	0.79	44	2.41
Ca2Zr10	0.00	0.00	34	0.00

Ca2Zr10	0.26	0.21	34	1.34
Ca2Zr10	0.27	0.22	34	1.45
Ca2Zr10	0.45	0.36	34	2.83
Ca2Zr12	0.00	0.00	40	0.00
Ca2Zr12	0.04	0.07	40	0.57
Ca2Zr12	0.02	0.04	40	0.36
Ca2Zr12	0.14	0.07	40	1.61
Ca2Zr16	0.00	0.00	52	0.00
Ca2Zr16	0.42	0.05	52	7.04
Ca2Zr16	0.91	0.64	52	5.23
Ca2Zr16	0.99	0.71	52	5.35
Ca2Zr5	0.00	0.00	19	0.00
Ca2Zr5	0.01	0.10	19	4.74
Ca2Zr5	0.23	0.19	19	2.40
Ca2Zr5	0.24	0.21	19	1.59
Ca2Zr8	0.00	0.00	28	0.00
Ca2Zr8	0.63	0.59	28	1.69
Ca2Zr8	0.82	0.78	28	1.25
Ca2Zr8	0.82	0.80	28	0.71
Ca4Zr12	0.00	0.00	44	0.00
Ca4Zr12	0.26	0.31	44	0.92
Ca4Zr12	0.52	0.59	44	1.49
Ca4Zr12	0.74	0.68	44	1.34
Ca4Zr4	0.00	0.00	20	0.00
Ca4Zr4	0.12	0.09	20	1.93
Ca4Zr4	0.24	0.28	20	2.08
Ca4Zr4	0.31	0.38	20	3.63
Ca4Zr5	0.00	0.00	23	0.00
Ca4Zr5	0.01	0.18	23	7.71
Ca4Zr5	0.07	0.20	23	5.42
Ca4Zr5	0.06	0.15	23	3.86
Ca4Zr6	0.00	0.00	26	0.00
Ca4Zr6	0.19	0.25	26	2.16
Ca4Zr6	0.28	0.32	26	1.59
Ca4Zr6	0.21	0.28	26	2.68
Ca4Zr8	0.00	0.00	32	0.00
Ca4Zr8	0.00	0.11	32	4.41
Ca4Zr8	0.45	0.33	32	3.52
Ca4Zr8	0.38	0.42	32	1.08
Ca4Zr9	0.00	0.00	35	0.00

Ca4Zr9	0.17	0.15	35	0.57
Ca4Zr9	0.50	0.46	35	1.25
Ca4Zr9	0.78	0.69	35	2.78
Ca6Zr4	0.00	0.00	24	0.00
Ca6Zr4	0.00	0.12	24	5.29
Ca6Zr4	0.28	0.38	24	3.98
Ca6Zr4	0.37	0.33	24	1.51
Ca8Zr4	0.00	0.00	28	0.00
Ca8Zr4	0.69	0.71	28	0.79
Ca8Zr4	0.68	0.66	28	0.73
Ca8Zr4	0.92	0.91	28	0.53
Ca9Zr4	0.00	0.00	30	0.00
Ca9Zr4	0.48	0.44	30	1.24
Ca9Zr4	0.47	0.49	30	0.74
Ca9Zr4	0.47	0.51	30	1.41
CaZr10	0.00	0.00	32	0.00
CaZr10	0.20	0.17	32	0.94
CaZr10	0.07	0.12	32	1.56
CaZr10	0.21	0.29	32	2.69
RMSE				2.48

Table S4b. Benchmark of NN+D3 against DFT+D3 relative energies for NaZrO structures.

Name	**DFT+D3**	**NN+D3**	**Natom**	**Err(meV/atom)**
Na2Zr18	0.00	0.00	57	0.00
Na2Zr18	1.25	1.26	57	0.15
Na2Zr18	1.54	1.31	57	3.99
Na2Zr18	1.42	1.30	57	2.18
Na2Zr24	0.00	0.00	75	0.00
Na2Zr24	0.07	0.05	75	0.17
Na2Zr24	0.10	0.02	75	1.00
Na2Zr24	0.20	0.22	75	0.20
Na2Zr36	0.00	0.00	111	0.00
Na2Zr36	0.18	0.11	111	0.68
Na2Zr36	0.11	0.14	111	0.30
Na2Zr36	0.34	0.34	111	0.03
Na4Zr10	0.00	0.00	36	0.00
Na4Zr10	0.37	0.42	36	1.34
Na4Zr10	0.38	0.51	36	3.58

Table S4b. Benchmark of NN+D3 against DFT+D3 relative energies for NaZrO structures.

Name	DFT+D3	NN+D3	Natom	Err(meV/atom)
Na4Zr10	0.31	0.49	36	4.96
Na4Zr11	0.00	0.00	39	0.00
Na4Zr11	0.01	0.09	39	2.10
Na4Zr11	0.09	0.18	39	2.41
Na4Zr11	0.33	0.49	39	3.41
Na4Zr12	0.00	0.00	42	0.00
Na4Zr12	0.06	0.04	42	0.51
Na4Zr12	0.11	0.18	42	1.81
Na4Zr12	0.11	0.10	42	0.23
Na4Zr2	0.00	0.00	12	0.00
Na4Zr2	0.56	0.53	12	1.87
Na4Zr2	0.50	0.45	12	4.66
Na4Zr2	0.48	0.43	12	3.73
Na4Zr3	0.00	0.00	15	0.00
Na4Zr3	0.58	0.47	15	7.32
Na4Zr3	0.65	0.56	15	5.67
Na4Zr3	0.75	0.63	15	7.94
Na4Zr4	0.00	0.00	18	0.00
Na4Zr4	0.27	0.16	18	5.77
Na4Zr4	0.25	0.25	18	0.15
Na4Zr4	0.22	0.26	18	2.42
Na4Zr5	0.00	0.00	21	0.00
Na4Zr5	0.64	0.66	21	0.69
Na4Zr5	0.66	0.71	21	2.09
Na4Zr5	0.66	0.70	21	2.15
Na4Zr6	0.00	0.00	24	0.00
Na4Zr6	0.18	0.10	24	3.42
Na4Zr6	0.16	0.15	24	0.68
Na4Zr6	0.31	0.23	24	3.51
Na4Zr7	0.00	0.00	27	0.00
Na4Zr7	0.09	0.04	27	1.71
Na4Zr7	0.15	0.08	27	2.51
Na4Zr7	0.23	0.06	27	6.28
Na4Zr8	0.00	0.00	30	0.00
Na4Zr8	0.00	0.00	30	0.00
Na4Zr8	0.00	0.00	30	0.00
Na4Zr8	0.17	0.06	30	3.67
Na4Zr9	0.00	0.00	33	0.00

Table S4b. Benchmark of NN+D3 against DFT+D3 relative energies for NaZrO structures.

Name	DFT+D3	NN+D3	Natom	Err(meV/atom)
Na4Zr9	0.40	0.27	33	3.83
Na4Zr9	0.54	0.44	33	3.05
Na4Zr9	0.64	0.60	33	1.15
Na6Zr2	0.00	0.00	15	0.00
Na6Zr2	0.83	0.69	15	9.35
Na6Zr2	0.81	0.68	15	9.04
Na6Zr2	0.80	0.68	15	8.36
Na8Zr2	0.00	0.00	18	0.00
Na8Zr2	0.19	0.14	18	2.74
Na8Zr2	0.28	0.32	18	2.10
Na8Zr2	0.30	0.29	18	0.44
RMSE				3.28

Table S4c. Benchmark of NN+D3 against DFT+D3 relative energies for KZrO structures.

Name	DFT+D3	NN+D3	Natom	Err(meV/atom)
K2Zr16	0.00	0.00	51	0.00
K2Zr16	0.33	0.47	51	5.33
K2Zr16	0.83	0.93	51	4.03
K2Zr16	0.99	1.23	51	9.71
K4Zr10	0.00	0.00	72	0.00
K4Zr10	0.66	0.83	72	2.37
K4Zr10	0.83	1.00	72	2.31
K4Zr10	1.30	1.40	72	1.38
K4Zr12	0.00	0.00	84	0.00
K4Zr12	0.01	0.01	84	0.01
K4Zr12	0.51	0.39	84	1.48
K4Zr12	0.27	0.34	84	0.89
K4Zr2	0.00	0.00	24	0.00
K4Zr2	0.07	0.02	24	2.24
K4Zr2	0.06	0.04	24	1.10
K4Zr2	0.08	0.06	24	0.45
K4Zr3	0.00	0.00	30	0.00
K4Zr3	0.04	0.04	30	0.23
K4Zr3	0.05	0.05	30	0.01
K4Zr3	0.20	0.11	30	2.81
K4Zr4	0.00	0.00	36	0.00

Table S4c. Benchmark of NN+D3 against DFT+D3 relative energies for KZrO structures.

Name	DFT+D3	NN+D3	Natom	Err(meV/atom)
K4Zr4	0.03	0.02	36	0.07
K4Zr4	0.07	0.05	36	0.50
K4Zr4	0.19	0.09	36	2.70
K4Zr6	0.00	0.00	48	0.00
K4Zr6	0.42	0.24	48	3.88
K4Zr6	0.53	0.53	48	0.15
K4Zr6	0.69	0.66	48	0.74
K4Zr8	0.00	0.00	60	0.00
K4Zr8	0.12	0.01	60	1.83
K4Zr8	0.14	0.01	60	2.12
K4Zr8	0.15	0.39	60	3.94
K6Zr2	0.00	0.00	30	0.00
K6Zr2	0.10	0.07	30	0.97
K6Zr2	0.27	0.25	30	0.43
K6Zr2	0.34	0.21	30	4.26
K8Zr2	0.00	0.00	36	0.00
K8Zr2	0.71	0.44	36	7.28
K8Zr2	0.79	0.60	36	5.37
K8Zr2	0.92	0.78	36	3.71
RMSE				2.87

Table S4d. Energy convergence tests of NaZrO structures with respect to K-point density and force criterion.

Name	Eref (eV)	K=35(eV)	ΔK-35 (meV/atom)	F=0.01(eV)	F=0.01/(meV/atom)
Na8Zr2	-108.8461	-108.8463	0.02	-108.8493	0.18
Na6Zr2	-97.2991	-97.2992	0.01	-97.3008	0.12
Na4Zr2	-85.5060	-85.5073	0.11	-85.5077	0.14
Na4Zr3	-113.6305	-113.6306	0.01	-113.6333	0.18
Na4Zr4	-143.2655	-143.2653	0.01	-143.2653	0.01
Na4Zr5	-172.3936	-172.3930	0.03	-172.3936	0.00
Na4Zr6	-201.1744	-201.1741	0.01	-201.1753	0.04
Na4Zr7	-229.8268	-229.8272	0.01	-229.8270	0.01
Na4Zr8	-259.2224	-259.2219	0.02	-259.2257	0.11
Na4Zr9	-288.4958	-288.4951	0.02	-288.4985	0.08
Na4Zr10	-317.2752	-317.2748	0.01	-317.2753	0.00
Na4Zr11	-346.1961	-346.1964	0.01	-346.1964	0.01
Na4Zr12	-374.6603	-374.6604	0.00	-374.6635	0.07
Na2Zr18	-535.9400	-535.9409	0.02	-535.9443	0.07

Na2Zr36	-1057.5997	-1057.5993	0.00	-1057.6132	0.12

5. Per-metal Formation Energy and Gibbs Free Energy of XZrO Systems

Table S5. Formation Energy and Free Energy (per metal/meV) of NaZrO

Chem.formula	ΔE/mev	ΔG-300/meV	ΔG-400/meV	ΔG-700/meV	ΔG-1000/meV	GM
Na8Zr2	-258	-288	-322	-446	-593	Zr-6c
Na6Zr2	-382	-414	-447	-566	-707	Zr-6c
Na4Zr2	-548	-591	-624	-739	-875	Zr-6c
Na4Zr3	-331	-370	-398	-499	-618	Zr-6c
Na4Zr4	-358	-415	-446	-552	-675	Zr-6c
Na4Zr5	-322	-385	-415	-518	-640	Zr-6c
Na4Zr6	-259	-307	-333	-419	-521	Zr-6c
Na4Zr7	-196	-227	-247	-317	-402	Zr-6c
Na4Zr8	-255	-280	-298	-360	-437	Zr-6c
Na4Zr9	-203	-230	-247	-306	-380	Zr-6c
Na4Zr10	-165	-201	-239	-254	-357	Zr-6c
Na4Zr11	-144	-172	-188	-244	-314	Zr-6c
Na4Zr12	-96	-135	-153	-215	-290	Zr-6c
Na2Zr10	-44	-97	-118	-171	-236	t
Na2Zr18	-14	-53	-66	-111	-166	t
Na2Zr24	19	-4	-13	-33	-66	m
Na2Zr36	44	25	18	-6	-39	m

Table S6. Formation Energy and Free Energy (per metal/meV) of KZrO

Chem.formula	ΔE/mev	ΔG-300/meV	ΔG-400/meV	ΔG-900/meV	ΔG-1000/meV	GM
K2Zr36	74	49	44	16	11	m
K2Zr18	17	-22	-31	-74	-83	m
K2Zr16	-12	-75	-91	-147	-160	t
K2Zr14	7	-52	-67	-142	-158	t
K2Zr12	48	-7	-20	-86	-100	t
K2Zr10	-19	-78	-93	-161	-174	Zr-6c
K2Zr8	17	-60	-79	-171	-190	Zr-6c
K4Zr12	-80	-140	-154	-224	-237	Zr-6c
K4Zr10	-192	-259	-275	-351	-366	Zr-6c
K4Zr8	-263	-359	-382	-492	-513	Zr-6c
K4Zr6	-224	-311	-332	-432	-452	Zr-6c
K4Zr4	-432	-523	-545	-650	-670	Zr-6c
K4Zr3	-428	-539	-566	-696	-721	Zr-6c
K4Zr2	-463	-564	-588	-706	-729	Zr-6c

K6Zr2	-287	-411	-440	-579	-606	Zr-6c
K8Zr2	-325	-460	-492	-650	-681	Zr-6c

Table S7. Formation Energy and Free Energy (per metal/meV) of CaZrO

Chem.formula	ΔE/mev	ΔG-300/meV	ΔG-400/meV	ΔG-900/meV	ΔG-1000/meV	GM
CaZr10	61	-24	-22	-71	43	m
Ca2Zr16	20	-6	-12	-160	-49	t
Ca2Zr12	8	-22	-29	-181	-72	t
Ca2Zr10	-27	-59	-66	-220	-114	t
Ca2Zr8	-61	-95	-104	-259	-154	t
Ca4Zr12	-28	-62	-70	-223	-121	t
Ca2Zr5	-46	-77	-84	-235	-134	t
Ca4Zr9	-47	-79	-86	-233	-132	t
Ca4Zr8	-26	-50	-56	-192	-90	t
Ca4Zr6	-44	-58	-70	-263	-168	Zr-6c
Ca4Zr5	-28	-49	-54	-180	-83	Zr-6c
Ca4Zr4	-125	-165	-175	-324	-234	Zr-6c
Ca6Zr4	-62	-96	-105	-243	-156	Zr-6c
Ca8Zr4	-109	-124	-127	-238	-150	Zr-6c
Ca9Zr4	-50	-69	-73	-188	-102	Zr-6c
Ca10Zr4	-51	-67	-72	-182	-97	Zr-6c
Ca12Zr4	-8	-26	-30	-142	-58	Zr-6c
Ca14Zr4	-8	-33	-39	-158	-77	Zr-6c
Ca16Zr4	2	-26	-33	-154	-75	Zr-6c

6. Bader charge analysis of $ZrO_{1.69}$

Table S8. Bader charge analysis of $ZrO_{1.69}$

	X_coordinate	Y_coordinate	Z_coordinate	Bader Charge
Zr	6.56	3.13	2.54	2.29
Zr	7.49	3.87	5.94	2.29
Zr	5.52	1.04	5.20	2.27
Zr	4.22	0.50	2.10	2.27
Zr	4.29	5.51	0.91	2.24
Zr	8.78	0.61	3.78	2.18
Zr	1.71	3.14	0.43	2.18
Zr	8.04	0.51	0.35	2.16

Zr	0.89	1.06	3.01	2.16
Zr	4.94	5.93	4.27	2.08
Zr	10.14	3.00	1.67	1.92
Zr	11.09	-1.38	5.11	1.75
Zr	8.92	5.62	3.23	1.69
Zr	11.98	5.64	2.21	1.49
Zr	11.28	3.82	4.63	1.42
Zr	2.71	3.79	3.46	1.41
O	5.09	1.99	3.36	-1.11
O	4.26	-0.27	4.07	-1.11
O	7.80	6.75	1.77	-1.12
O	3.70	1.83	5.89	-1.15
O	6.10	4.37	0.73	-1.16
O	10.29	6.97	2.20	-1.16
O	4.68	4.45	2.81	-1.17
O	1.47	2.43	4.55	-1.17
O	2.35	4.91	1.58	-1.17
O	8.27	1.84	2.05	-1.17
O	7.05	4.70	3.89	-1.18
O	9.45	0.13	5.72	-1.18
O	11.97	6.97	0.29	-1.18
O	11.37	4.31	0.53	-1.19
O	8.57	4.39	1.47	-1.19
O	1.46	-0.17	4.87	-1.19
O	10.42	2.11	3.60	-1.19
O	10.71	-0.35	3.20	-1.19
O	11.70	1.54	1.09	-1.19
O	2.24	-0.57	2.37	-1.20
O	5.84	7.03	0.17	-1.20
O	7.41	2.17	4.53	-1.20
O	5.83	1.66	0.94	-1.20
O	7.01	-0.41	4.61	-1.20
O	9.34	4.64	5.27	-1.21
O	2.67	2.05	2.03	-1.21
O	3.28	4.74	5.35	-1.23

7. **Thermodynamic data for HZrO systems**

Table S9. Thermodynamic data for HZrO systems.

Chemistry Formula	H molar content	E_t (meV/f.u.)	T/K*
H2Zr18-t	10.0%	90	968
H2Zr18-m	10.0%	0	/

Table S10. Comparison of zero-point energies and vibrational entropies at 1000 K obtained from the harmonic approximation and MD-based VACF sampling. The MD simulation is performed for 1ns using the Nosé–Hoover thermostat based on 2 × 2 × 2 supercells. The vibrational spectra are obtained from the Fourier transform of the velocity autocorrelation functions (VACFs), from which the

zero-point energies and vibrational entropies are derived.

System	Phase	ZPE (eV) Harmonic	ZPE (eV) MD	ΔZPE	S (J·mol⁻¹·K⁻¹) Harmonic	S (J·mol⁻¹·K⁻¹) MD	ΔS per Zr
ZrO_2	m	0.21	0.21	−0.01	128	133	+1.3
ZrO_2	t	0.20	0.20	−0.01	135	141	+1.5
$H_2Zr_{18}O_{37}$	m	4.48	4.34	−0.14	2407	2509	+5.7
$H_2Zr_{18}O_{37}$	t	4.28	4.18	−0.10	2537	2618	+4.5
$a_2Zr_{18}O_{37}$	t	3.78	3.75	−0.04	2590	2654	+3.6

8. Supplementary Figures of the NN potential test and NaZrO System

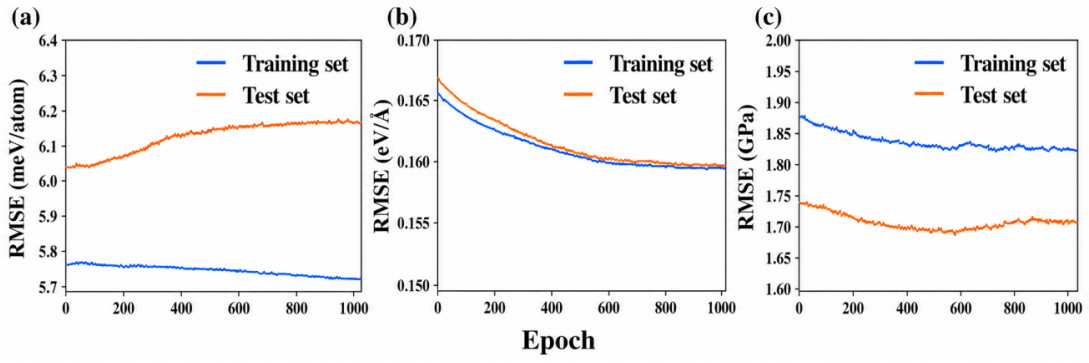

Fig. S1. Learning curve of the CaZrO neural network potential. (a) Energy training results. (b) Force training results. (c) Stress training results.

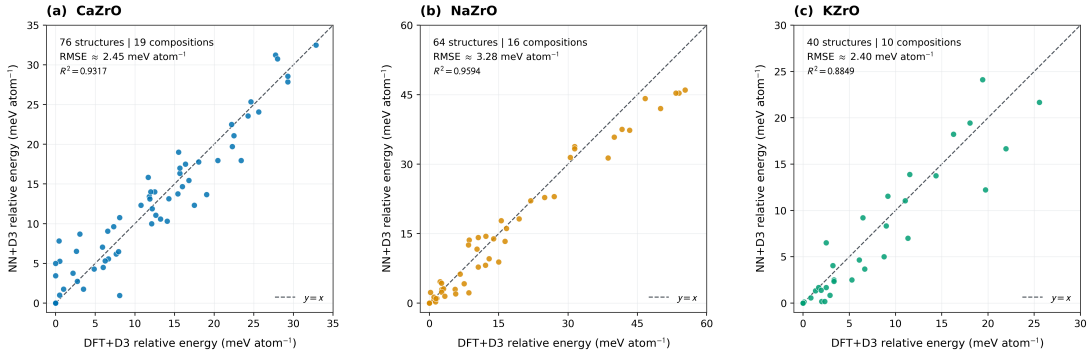

Fig. S2. Comparison of NN+D3 and DFT+D3 relative energies for (a) CaZrO, (b) NaZrO, and (c) KZrO using the structures listed in Tables S4a–c. Each point represents one structure, and dashed lines indicate y = x. Energies are normalized by the tabulated atom counts; N = 51 is used for $K_2Zr_{16}O_{33}$. RMSE and R^2 are calculated from the tabulated, rounded energies, with DFT as the reference. Energy zeros follow the source tables.

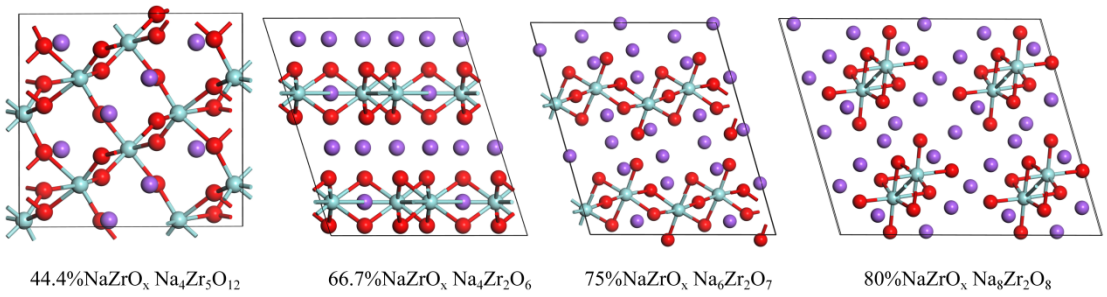

Fig. S3. Atomic structures of $Na_4Zr_5O_{12}$ (44.4% Na), $Na_4Zr_2O_6$ (66.7% Na) ,$Na_6Zr_2O_7$ (75% Na), and $Na_8Zr_2O_8$ (80% Na). Cyan spheres represent Zr atoms, purple spheres represent Na atoms, and red spheres represent O atoms.

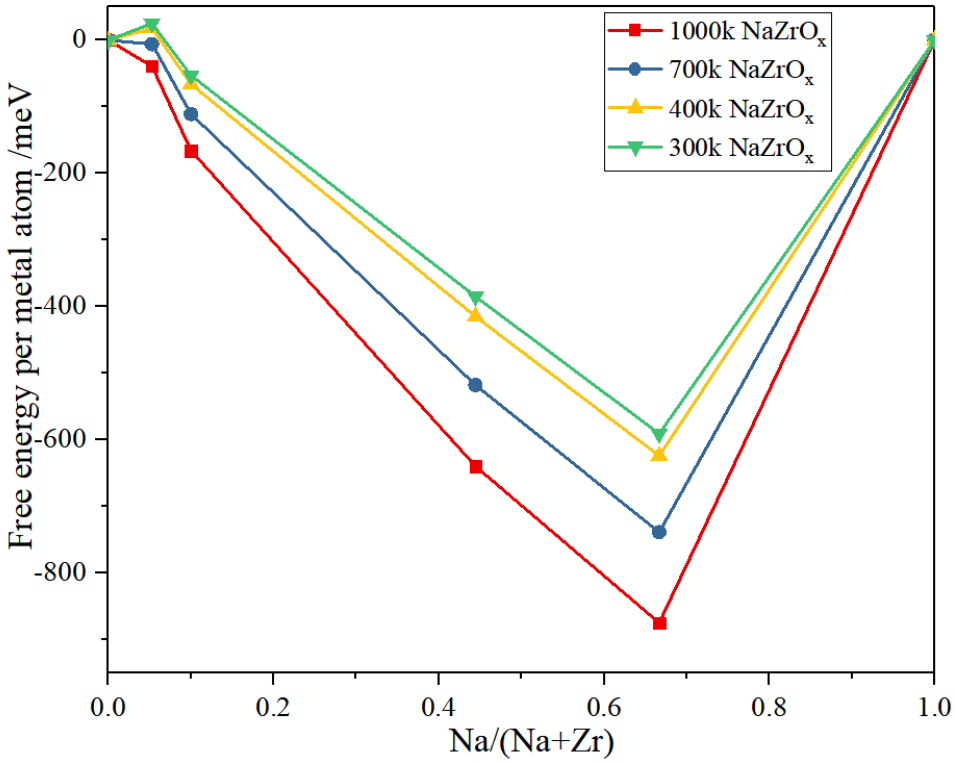

Fig. S4. Thermodynamic diagram of the main NaZrO structures at different temperatures, including compositions with 5.3%, 10%, 45.4%, and 66.7% Na. The x-axis represents the Na molar fraction, and the y-axis shows the Gibbs free energy per metal atom (in meV). Data are shown for 1000 K (red), 900 K (blue), 400 K (yellow), and 300 K (green).

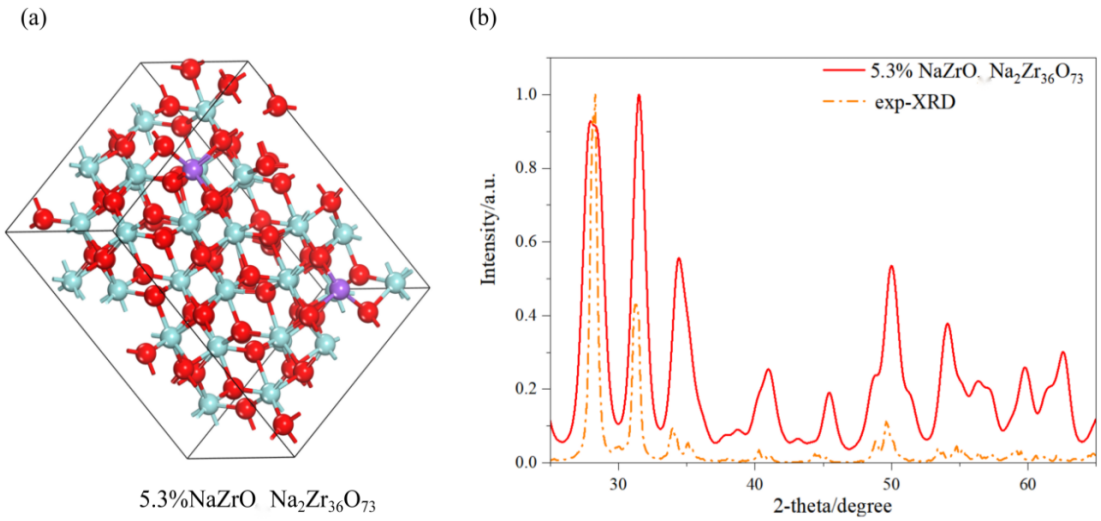

Fig. S5. (a) Atomic structure of 5.3% NaZrO ($Na_2Zr_{36}O_{73}$). Cyan spheres represent Zr atoms, purple spheres represent Na atoms, and red spheres represent O atoms. (b) Simulated XRD pattern of $Na_2Zr_{36}O_{73}$ with peak width = 1(red line) and experimental XRD (orange line)

9. Supplementary Figures of the KZrO System

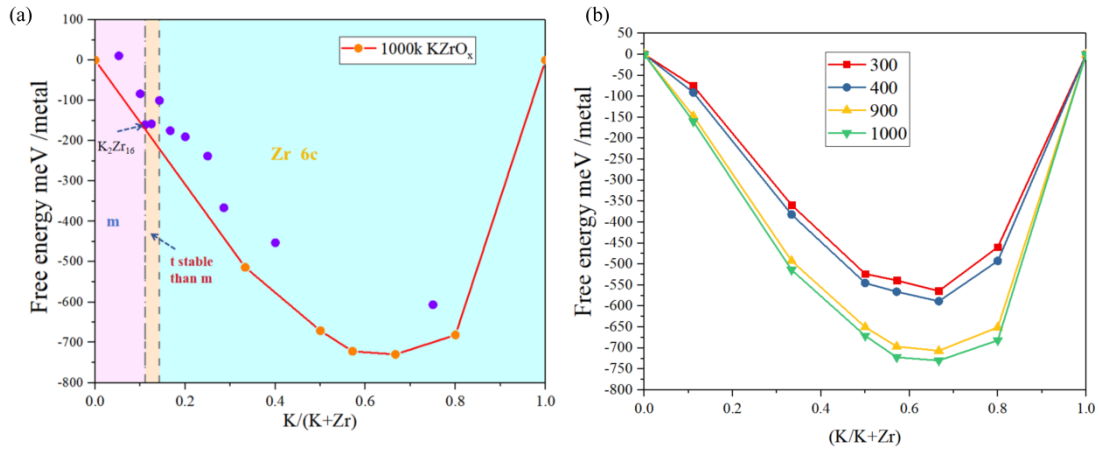

Fig. S6. (a) The per-metal atom Gibbs free energy phase diagram of the K_2O-ZrO_2 system at 1000 K. The y-axis represents the formation Gibbs free energy, and the x-axis represents the molar percentage of K content . The orange points along the line represent the convex points of the system and purple points is not convex points.In the range of 0-11.1% (pink area), the monoclinic phase (m-ZrO_2) is more stable than the tetragonal phase (t-ZrO_2). In the range of 11.1%-14.3%(yellow area), the tetragonal phase is more stable than the monoclinic phase. When the K content exceeds 14.3% (blue area), the GM structures at different compositions begin to exhibit six-coordinated Zr atoms. (b)Thermodynamic diagram of the main $KZrO_x$ structures at different temperatures. The x-axis represents the K molar fraction, and the y-axis shows the Gibbs free energy per metal atom (in meV). Data are shown for 300 K (red), 400 K (blue), 900 K (yellow), and 1000 K (green).

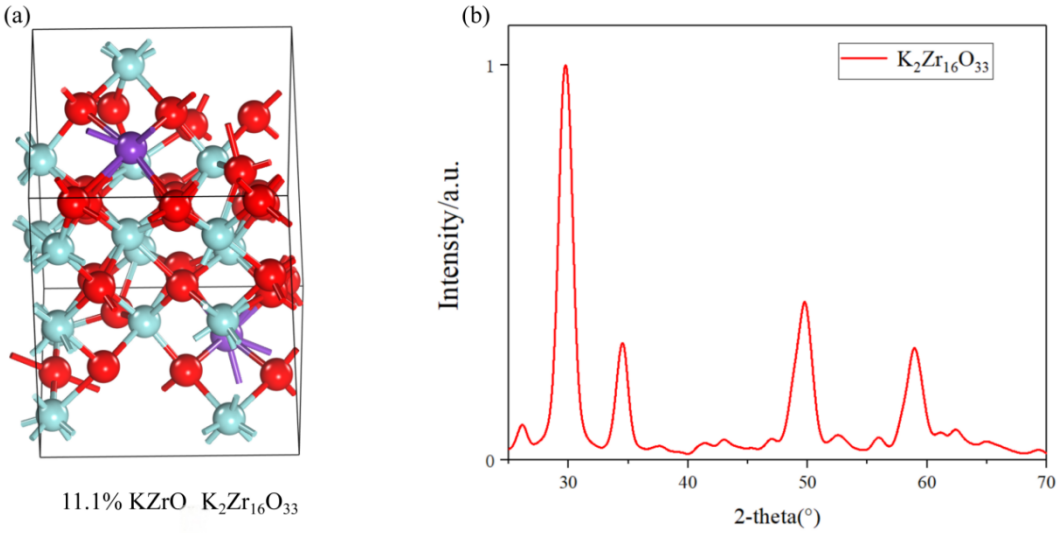

Fig. S7. (a) Atomic structure of 11.1% KZrO ($K_2Zr_{16}O_{33}$). Cyan spheres represent Zr atoms, purple spheres represent K atoms, and red spheres represent O atoms. (b) Simulated XRD pattern of $K_2Zr_{16}O_{33}$ with peak width = 1.

10. Supplementary Figures for HZrO and KZrO

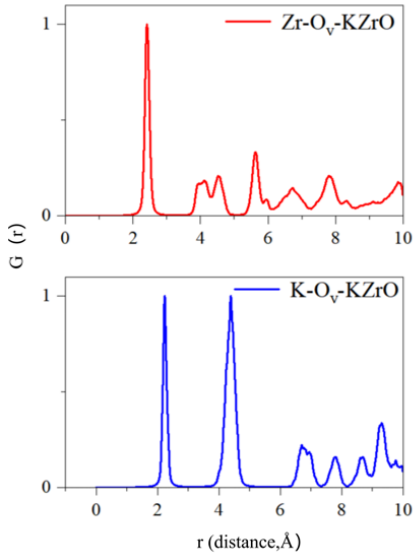

Fig. S8 Radial distribution functions (RDFs) of formal oxygen vacancies in the $K_2Zr_{16}O_{33}$. The x-axis denotes the distance (Å), and the y-axis denotes the normalized distribution intensity.

11. Supplementary Figures of the CaZrO System

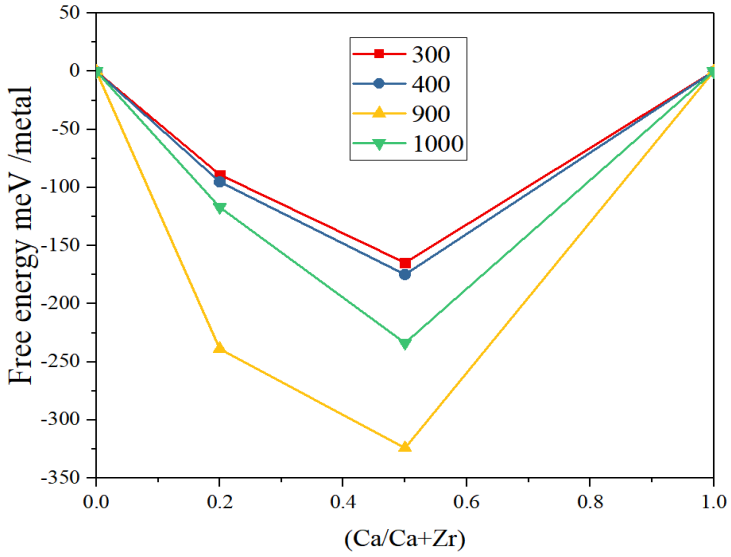

Fig. S9. Thermodynamic diagram of the main $CaZrO_x$ structures at different temperatures (20%CaZrO and 50%CaZrO). The x-axis represents the Ca molar fraction, and the y-axis shows the Gibbs free energy per metal atom (in meV). Data are shown for 300 K (red), 400 K (blue), 900 K (yellow), and 1000 K (green).

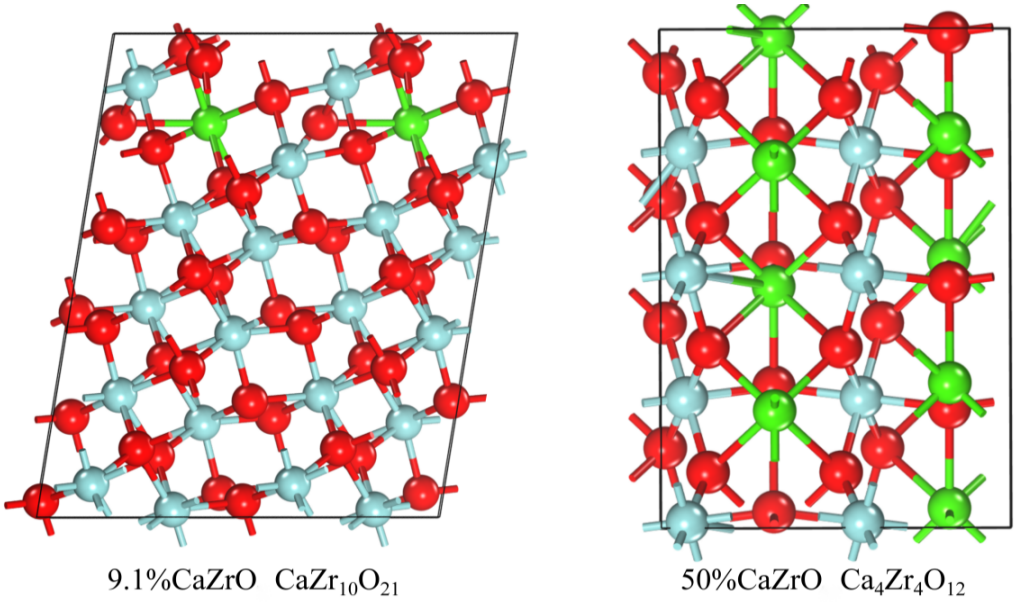

Fig. S10. Atomic structures of $CaZr_{10}O_{21}$ (9.1% Ca) and $Ca_4Zr_4O_{12}$ (50% Ca) Cyan spheres represent Zr atoms, green spheres represent Ca atoms, and red spheres represent O atoms.

12. Supplementary Figures for MgZrO system

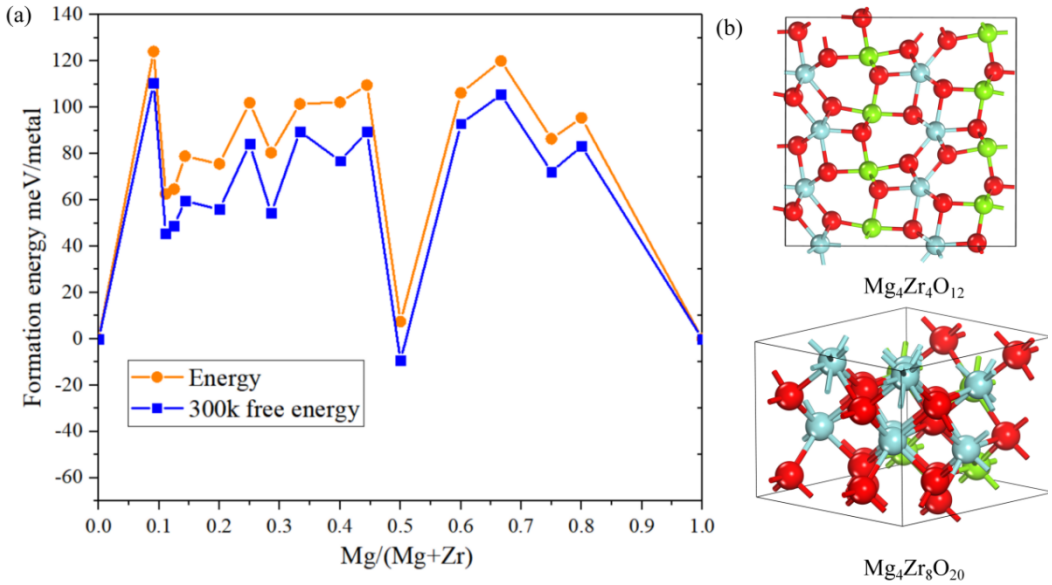

Fig. S11 (a) Phase diagram of the MgZrO system. The x-axis shows the molar fraction of Mg (mol%), and the y-axis shows the per-metal-atom formation energy of MgZrO (meV). The orange curve corresponds to the formation energy (Energy), and the blue curve corresponds to the formation free energy at 300 K (b) Representative structures of the MgZrO system. Green, red, and blue spheres represent Mg, O, and Zr, respectively.

13. Supplementary Figures of HZrO System

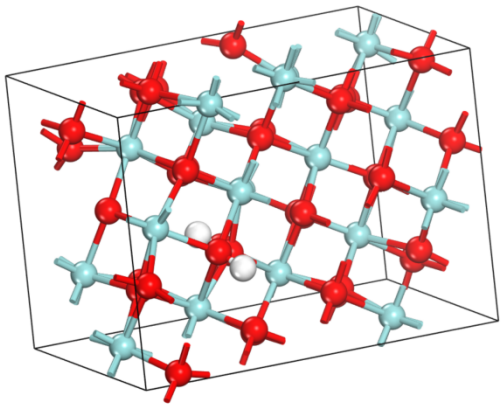

$H_2Zr_{18}O_{37}$

Fig. S12 Atomic structures of $H_2Zr_{18}O_{37}$.Cyan spheres represent Zr atoms, white spheres represent H ,and red spheres represent O atoms.

14. Supplementary Figures of the ZrO_{2-x} System

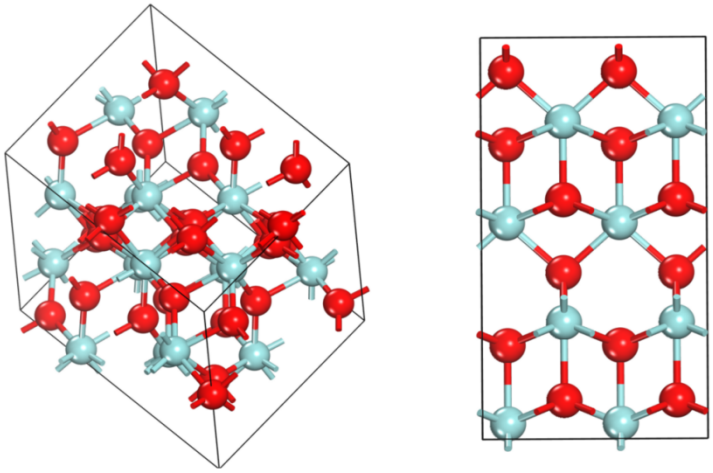

25% Zr^{3+} $ZrO_{1.88}$ 100% Zr^{3+} $ZrO_{1.5}$

Fig. S13 Atomic structures of ZrO1.88 (25%Zr^{3+}) and Zr_2O_3 (100% Zr^{3+}) Cyan spheres represent Zr atoms, and red spheres represent O atoms.

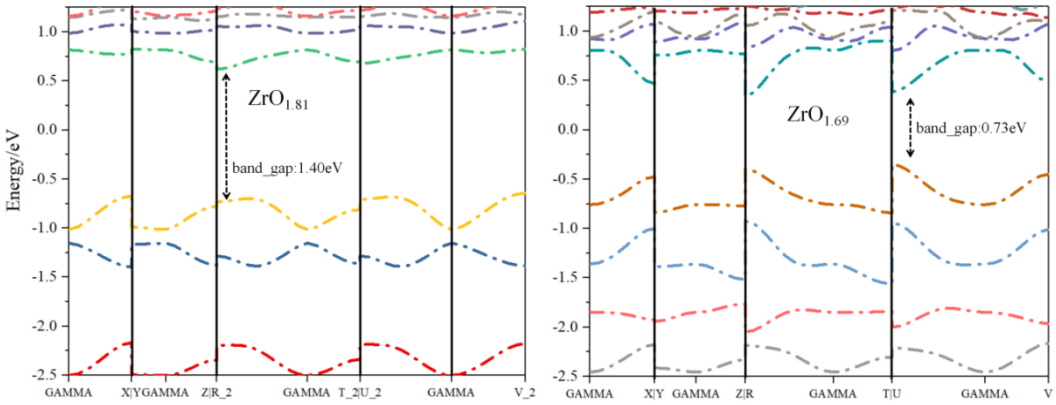

Fig. S14 Band structures of $ZrO_{1.81}$ (left) and $ZrO_{1.69}$ (right), with the Fermi level set to 0 eV in each case.

.

15. The formation energy calculations of XZrO solution

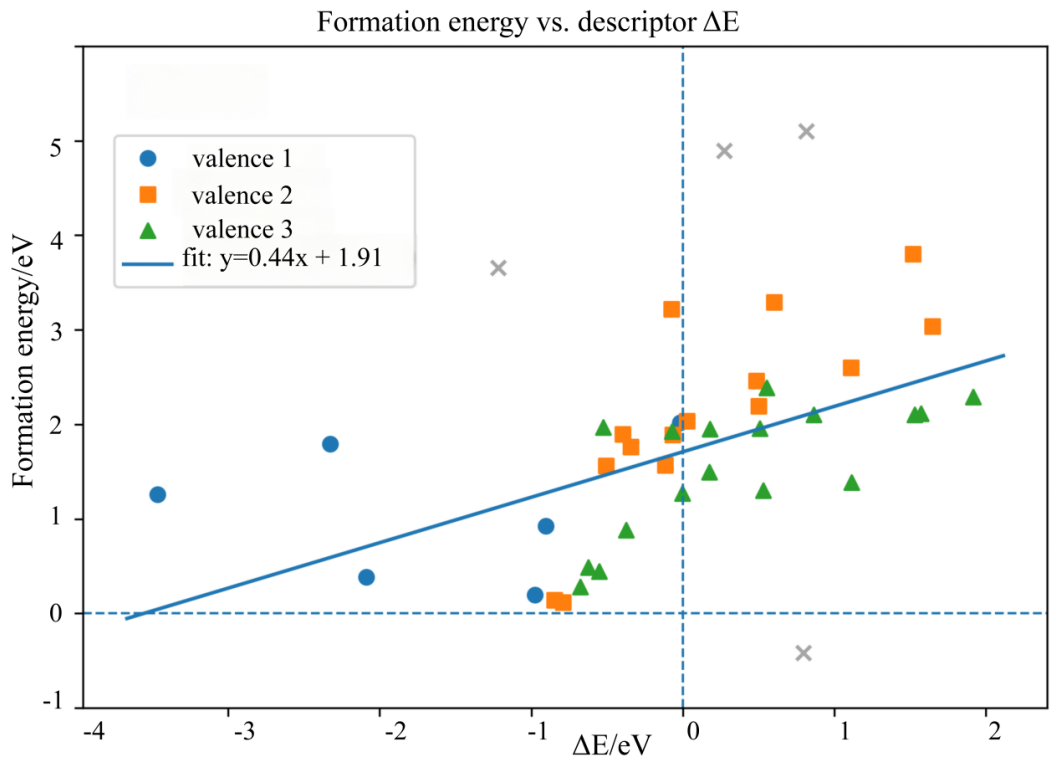

Fig. S15 ΔE–E_f correlation plot, with ΔE (defined in Section 3.5) in eV on the x-axis and E_f in eV on the y-axis. Monovalent, divalent, and trivalent metals are shown as blue circles, yellow squares, and green triangles, respectively. The solid blue line represents an ordinary least-squares (OLS) fit obtained after excluding outliers (grey crosses) identified by $|r| > 2.5\ \sigma$ in an initial fit, where r is the residual and σ is estimated from the median absolute deviation (MAD).

16. Supplementary Figures for Experimental Characterization

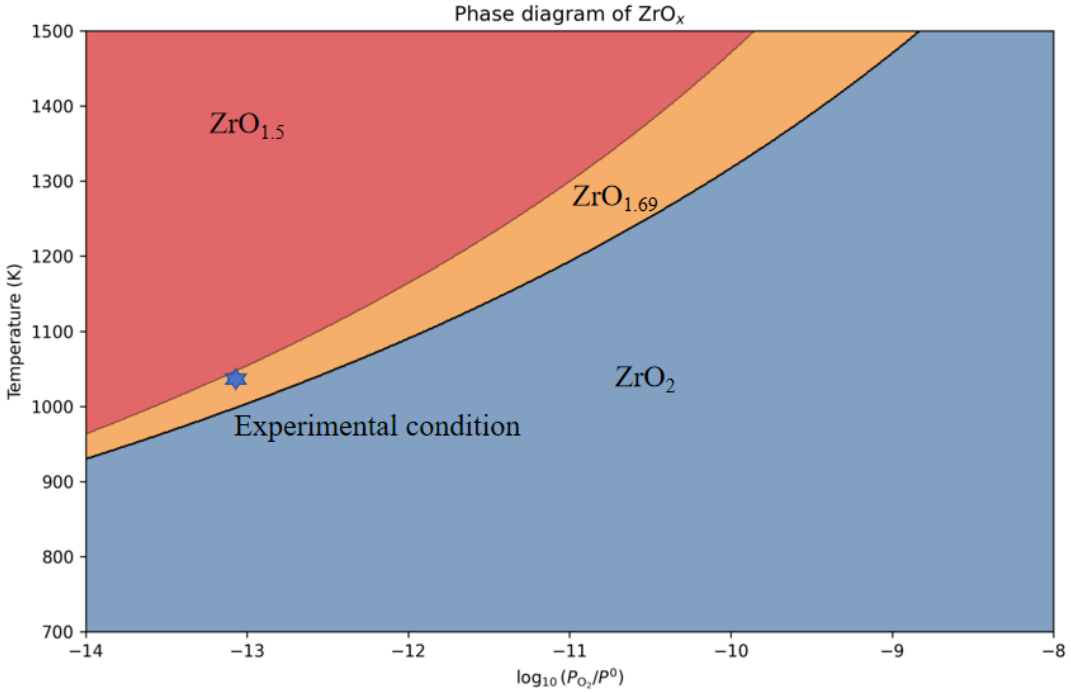

Fig. S16. Phase diagram of ZrO_{2-x} as a function of oxygen partial pressure (log10 P) and temperature (K). The oxygen chemical potential under the experimental condition is calculated using PH2O = 5×10^{-7} bar (high-purity N_2) at 1000 K, with μO = μ(H_2O) - μ(acac(H)). H_2O is assumed to exist in the gas phase with a standard molar entropy of 188.8 J mol^{-1} K^{-1}, whereas the standard entropy contribution of H in solid acac is approximated as zero.



Fig. S17. Digital photographs of HSGZ and SGZ samples treated under different atmospheres. The top row shows the as-prepared samples, the middle row shows samples calcined in air (HSGZ-air and SGZ-air), and the bottom row shows samples calcined under N_2 atmosphere (HSGZ-N_2 and SGZ-N_2).

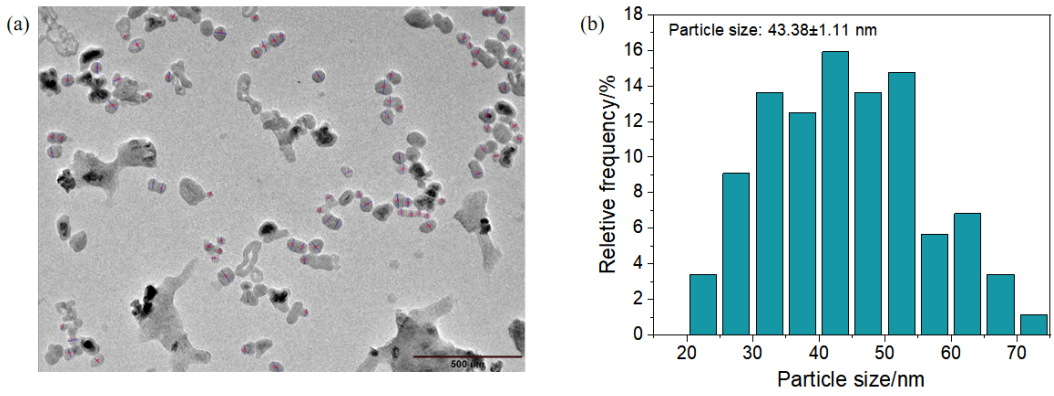

Fig. S18. (a) TEM image of CaZrO after calcination at 1100 °C. (b) Nanoparticle size distribution of CaZrO-1100.

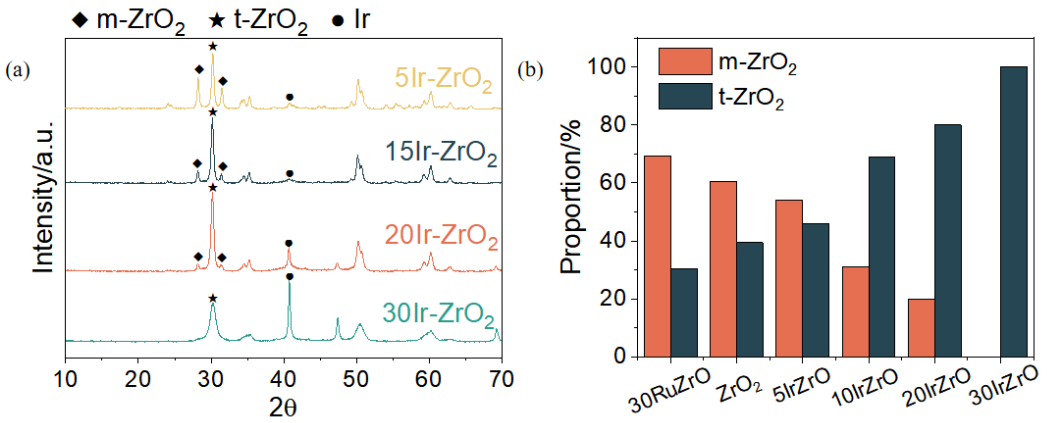

Fig. S19. (a) XRD patterns of IrZrO samples with different Ir contents: 5Ir-ZrO_2 (yellow), 15Ir-ZrO_2 (black), 20Ir-ZrO_2 (red), and 30Ir-ZrO_2 (green). (b) Quantified fractions of t-ZrO_2 (black) and m-ZrO_2 (orange) obtained from XRD analysis.

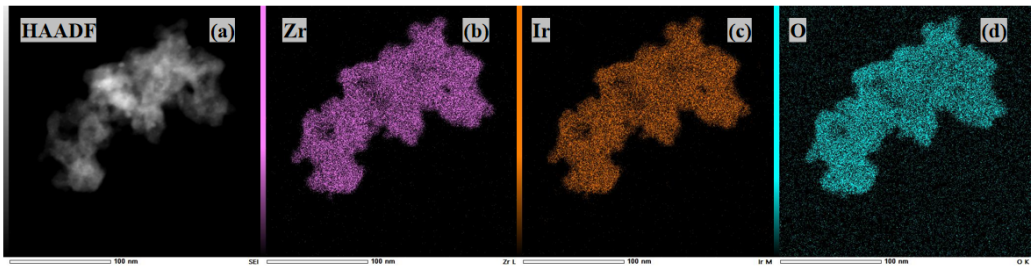

Fig. S20. HAADF-STEM(a) and EDS(b-d) images of 30% IrZrO

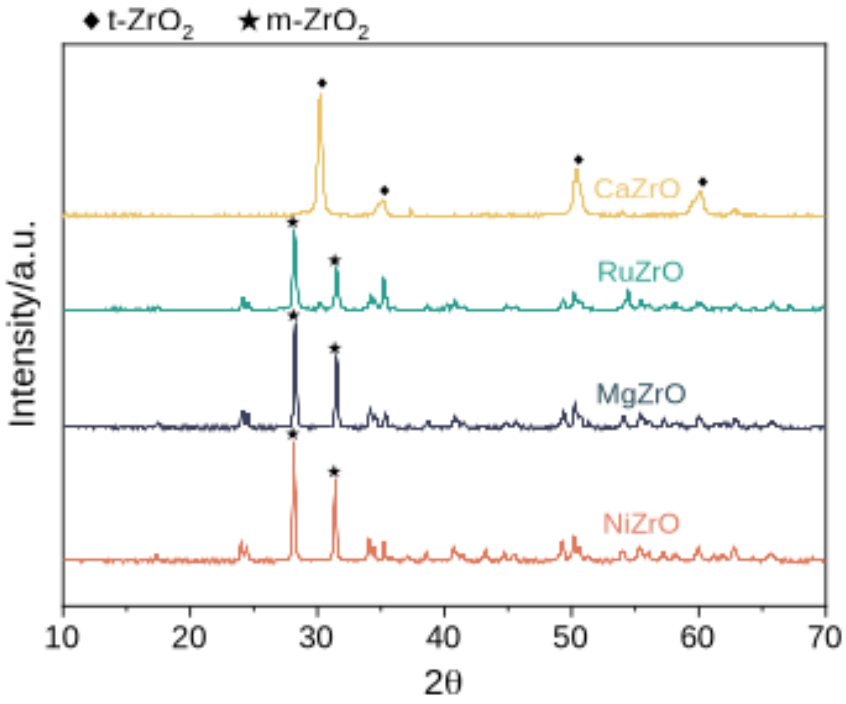

Fig. S21. XRD patterns of CaZrO (yellow), RuZrO (green), MgZrO (black), and NiZrO (red) after calcination at 1100 °C.

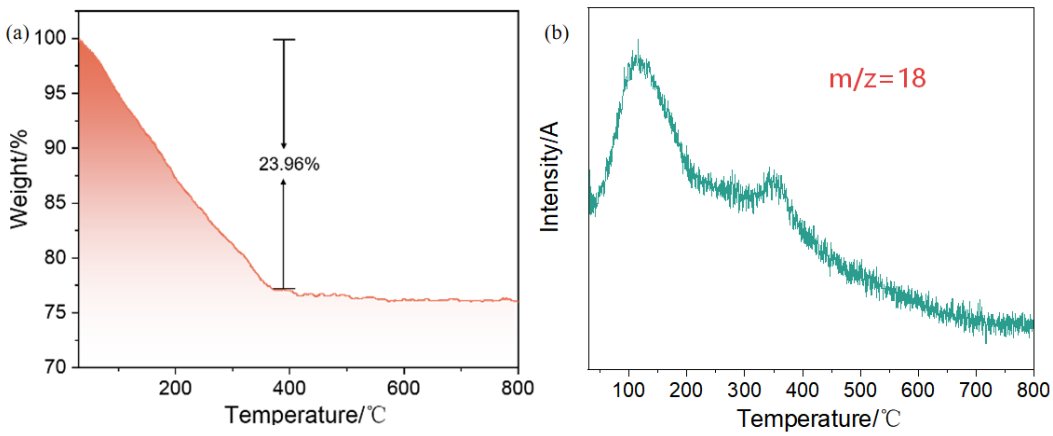

Fig. S22. (a) Thermogravimetric analysis of the slurry-like NaZrO precursor. (b) MS signal of H2O released during thermogravimetric mass loss.

17. Synthetic method

The IrZrO solid solution was synthesized via the solvothermal method. Firstly, 3.867 g $ZrOCl_2 \cdot 8H_2O$, 7.207 g urea and 0.3583 g $IrCl_3 \cdot xH_2O$ were weighted and dissolved in 30 mL methanol. Then, the solution was stirred at 40 ℃ for 30 min, and subsequently transferred into a 100 mL Teflon-lined autoclave. Afterward, the one-pot solvethermal synthesis was carried out at 160°C for 20 h in an electric oven. The obtained suspension was washed to neutrality, dried at 80 ℃ and ground into a fine powder. Finally, the as-prepared powder was reduced at 600 ℃ for 4 h (5%H_2/95%Ar). The synthetic method of other solid solutions was analogous to that of IrZrO, with the sole modification that $IrCl_3 \cdot xH_2O$ was repleaced by corresponding precursor.

Synthesis of t-ZrO_2 via the sol-gel method: First, 30 mL of n-propanol zirconium, 4.5 mL of Hacac, and 9 mL of n-propanol were measured out to prepare Solution A. 15 mL of deionized water and 16.5 mL of n-propanol were measured out to prepare Solution B. Slowly pour Solution A into Solution B. Stir the resulting suspension at 30 °C for 12 h, then dry and collect the yellow solid. Calcine the solid in air or nitrogen atmosphere at 600 °C for 1 h to obtain ZrO_2, designated as HSGZ. The synthesis method for SGZ is identical to that for HSGZ, except that Hacac is not added to Solution A.

18. Characterization

X-ray diffraction (XRD) patterns were obtained on a Bruker D8 using Cu (Kα = 0.15406 nm) as the X-ray source. The relative fraction of m-ZrO_2/t-ZrO_2 was estimated using a semiquantitative RIR method reported previously (Eq.1, 2).

$$W_m(\%) = \frac{I_m RIR_t}{I_t RIR_m + I_m RIR_t} \times 100 \quad (1)$$

$$W_t(\%) = 100 - W_m(\%) \quad (2)$$

Where W_m and W_t represent the witght proportion of m-ZrO_2 and t-ZrO_2, respectively, I_m and I_t are respectively the obtained integrated intensity of m-ZrO_2 and t-ZrO_2, and RIR_m and RIR_t are respevtively reference intensity ratios ofm-ZrO_2 and t-ZrO_2 to corundum (RIR_m=4.83 from PDF#83-0938, RIR_t=9.88 from PDF#79-1764).

Transmission electron microscopy (TEM) data were obtained on a FEI Tecnai G2 F20 S-TWIN transmission electron microscopy instrument operating at 200 kV.

The room temperature electron paramagnetic resonance (EPR) spectra were recorded on an EMXplus-6/1 (Bruker, Germany). And inductively coupled plasma mass spectrometry (ICP) was performed using the PE-8000 produced by PerkinElmer, USA.

Table S10 ICP analysis of Ir_2O_3-ZrO_2 system,The values in parentheses denote the molar percentage of Ir.

Materials	Zr: Ir (Theoretically)	Zr: Ir (Actually)
5Ir-ZrO_2	1:0.053(5%)	1:0.032(3.1%)
10Ir-ZrO_2	1:0.111(10%)	1:0.095(8.7%)
20Ir-ZrO_2	1:0.250(20%)	1:0.166(14.2%)
30Ir-ZrO_2	1:0.429(30%)	1:0.290(22.5%)

19. References

(1) Huang, S.-D.; Shang, C.; Zhang, X.-J.; Liu, Z.-P. Material Discovery by Combining Stochastic Surface Walking Global Optimization with a Neural Network. Chem. Sci. 2017, 8 (9), 6327-6337.

(2) Huang, S.-D.; Shang, C.; Kang, P.-L.; Liu, Z.-P. Atomic Structure of Boron Resolved Using Machine Learning and Global Sampling. Chem. Sci. 2018, 9 (46), 8644-8655.

(3) Huang, S.-D.; Shang, C.; Kang, P.-L.; Zhang, X.-J.; Liu, Z.-P. LASP: Fast Global Potential Energy Surface Exploration. WIREs Comput. Mol. Sci. 2019, 9 (6), e1415.

(4) Shang, C.; Liu, Z.-P. Stochastic Surface Walking Method for Structure Prediction and Pathway Searching. J. Chem. Theory Comput. 2013, 9 (3), 1838-1845.

(5) Zhang, X.-J.; Shang, C.; Liu, Z.-P. From Atoms to Fullerene: Stochastic Surface Walking Solution for Automated Structure Prediction of Complex Material. J. Chem. Theory Comput. 2013, 9 (7), 3252-3260.

(6) Shang, C.; Zhang, X.-J.; Liu, Z.-P. Stochastic Surface Walking Method for Crystal Structure and Phase Transition Pathway Prediction. Phys. Chem. Chem. Phys. 2014, 16 (33), 17845-17856.

(7) Shang, C.; Liu, Z.-P. Constrained Broyden Dimer Method with Bias Potential for Exploring Potential Energy Surface of Multistep Reaction Process. J. Chem. Theory Comput. 2012, 8 (7), 2215-2222.

(8) Xie, X.-T.; Yang, Z.-X.; Chen, D.; Shi, Y.-F.; Kang, P.-L.; Ma, S.; Li, Y.-F.; Shang, C.; Liu, Z.-P. LASP to the Future of Atomic Simulation: Intelligence and Automation. Precis. Chem. 2024.

(9) Ma, S.; Shang, C.; Liu, Z.-P. Heterogeneous Catalysis from Structure to Activity via SSW-NN Method. J. Chem. Phys. 2019, 151 (5), 050901.

(10) Shang, C.; Huang, S.-D.; Liu, Z.-P. Massively Parallelization Strategy for Material Simulation Using High-Dimensional Neural Network Potential. J. Comput. Chem. 2019, 40 (10), 1091-1096.

20. XYZ Coordinates of Key Structures

#10%NaZrOx $Na_2Zr_{18}O_{37}$

1.00000000000000

8.0936216292367096 0.0000000000000000 0.0000000000000000

-0.0228522084186716 8.1162628783572277 0.0000000000000000

1.3708744232677872 3.3945573649087004 10.2704695914363171

Na Zr O

2 18 37

Selective dynamics

Direct

0.4420140000000004	0.2696650000000034	0.6262580000000000	T	T	T
0.9864340000000027	0.8764180000000010	0.3692879999999974	T	T	T
0.7301509999999993	0.2681019999999990	0.8582490000000007	T	T	T
0.1015459999999990	0.0734819999999985	0.8504289999999983	T	T	T
0.9171199999999970	0.2755080000000021	0.1398930000000007	T	T	T
0.7560969999999969	0.4997359999999986	0.3694470000000010	T	T	T
0.1194360000000003	0.6383369999999999	0.1393180000000029	T	T	T
0.5254529999999988	0.4827879999999993	0.1090939999999989	T	T	T
0.3144569999999973	0.5058239999999969	0.8509349999999998	T	T	T
0.7769380000000012	0.8777860000000004	0.1113270000000028	T	T	T
0.4832400000000021	0.9113309999999970	0.8960760000000008	T	T	T
0.2176820000000035	0.8849909999999994	0.6222119999999975	T	T	T
0.6021849999999986	0.0942330000000027	0.3728539999999967	T	T	T
0.3514949999999999	0.0653689999999969	0.1463729999999970	T	T	T
0.8116679999999974	0.0389120000000034	0.6286660000000026	T	T	T
0.8841139999999967	0.6657539999999997	0.8790600000000026	T	T	T
0.6572079999999971	0.6433970000000002	0.6297420000000002	T	T	T
0.2043419999999969	0.2521910000000034	0.3681410000000014	T	T	T
0.3651359999999997	0.6605160000000012	0.3633459999999999	T	T	T
0.0641999999999996	0.4891119999999987	0.6287710000000004	T	T	T

0.7221249999999984 0.9015100000000018 0.5068619999999981 T T T

0.7057939999999974 0.2354819999999975 0.4895860000000027 T T T

0.4298259999999985 0.2323609999999974 0.2492250000000027 T T T

0.7008280000000013 0.7962259999999972 0.7562709999999981 T T T

0.5474809999999977 0.5573940000000022 0.4894439999999989 T T T

0.8681389999999993 0.5618270000000010 0.5127519999999990 T T T

0.5968349999999987 0.6515979999999999 0.2368230000000011 T T T

0.9295090000000030 0.2307539999999975 0.7173469999999966 T T T

0.9101339999999993 0.7124420000000029 0.2435639999999992 T T T

0.3106470000000030 0.9852330000000009 0.7580510000000018 T T T

0.2835949999999983 0.0270999999999972 0.9761680000000013 T T T

0.8422219999999996 0.5168559999999971 0.7537220000000033 T T T

0.3099630000000033 0.5064089999999979 0.2409219999999976 T T T

0.2083689999999976 0.3291809999999984 0.7735959999999977 T T T

0.1239530000000002 0.1425029999999978 0.2196039999999968 T T T

0.3727170000000015 0.0881899999999973 0.4930189999999968 T T T

0.7065890000000010 0.3501559999999984 0.2420260000000027 T T T

0.1885710000000032 0.7288250000000005 0.5013190000000023 T T T

0.2161680000000032 0.4104770000000002 0.4880259999999979 T T T

0.6759839999999997 0.7375910000000019 0.9968470000000025 T T T

0.0434630000000027 0.0598680000000016 0.5030689999999964 T T T

0.5859209999999990 0.0411199999999994 0.0206859999999978 T T T

0.2308909999999997 0.8132919999999970 0.2130659999999978 T T T

0.9146879999999982 0.1379170000000016 0.9871139999999983 T T T

0.9961160000000007 0.9171359999999993 0.7499490000000009 T T T

0.7389200000000002 0.4153519999999986 0.9967880000000022 T T T

0.3579829999999973 0.6651390000000035 0.9807550000000020 T T T

0.9909090000000020 0.8212019999999995 0.9944080000000000 T T T

0.1132210000000029 0.6382540000000034 0.7571220000000025 T T T

0.3935389999999970 0.3375139999999988 0.0191379999999981 T T T

0.7835960000000028 0.0377269999999967 0.2330979999999983 T T T

0.0564949999999982 0.4940890000000024 0.0091820000000027 T T T

0.4649969999999968 0.9136939999999996 0.3114929999999987 T T T

0.6320320000000024 0.1080680000000029 0.7630150000000029 T T T

0.5398399999999981 0.4200099999999978 0.7763130000000018 T T T

0.9994909999999990 0.4045660000000026 0.2780869999999993 T T T

0.4153799999999990 0.7124329999999972 0.6836959999999976 T T T

#66.7%NaZrO$_x$ Na$_4$Zr$_4$O$_{10}$

1.00000000000000

6.5215893086168331 0.0000000000000000 0.0000000000000000

1.5835680914786168 5.3544119174603413 0.0000000000000000

-1.5885699010659651 3.3782042176459699 4.1574008021158839

Na Zr O

4 2 6

Selective dynamics

Direct

0.1915130000000005	0.6773600000000002	0.1391360000000006	T	T	T
0.1914080000000027	0.0210409999999968	0.4823039999999992	T	T	T
0.6912829999999985	0.6775680000000008	0.1389160000000018	T	T	T
0.1915019999999998	0.3340359999999976	0.7955830000000006	T	T	T
0.6916060000000002	0.0096709999999973	0.4712650000000025	T	T	T
0.6914730000000020	0.3450419999999994	0.8070099999999982	T	T	T
0.9113720000000001	0.1666000000000025	0.6498589999999993	T	T	T
0.4746680000000012	0.8193449999999984	0.3623869999999982	T	T	T
0.9084599999999980	0.9004839999999987	0.2811980000000034	T	T	T
0.4717750000000009	0.1880379999999988	0.6284229999999980	T	T	T
0.9085049999999981	0.5353089999999980	0.9160040000000009	T	T	T
0.4746730000000028	0.4540509999999998	0.9972100000000026	T	T	T

#11.1% KZrO$_x$ K$_2$Zr$_{16}$O$_{33}$

1.00000000000000

10.8937934894104771	0.0000000000000000	0.0000000000000000
0.1001224450326134	7.4726817007103383	0.0000000000000000
-1.7899064356496546	-1.8337457288574024	7.7762167564710714

K	Zr	O
2	16	33

Selective dynamics

Direct

0.9212169999999986	0.5871339999999989	0.3840209999999971	T	T	T
0.1063860000000005	0.4507499999999993	0.7170970000000025	T	T	T
0.5609350000000006	0.5451400000000035	0.3565070000000006	T	T	T
0.2295549999999977	0.1246450000000010	0.3814040000000034	T	T	T
0.7732200000000020	0.4466589999999968	0.6929500000000033	T	T	T
0.3365840000000020	0.7407060000000030	0.0797629999999998	T	T	T
0.4905720000000002	0.9486220000000003	0.7265379999999979	T	T	T
0.6910280000000029	0.2971360000000018	0.0213779999999986	T	T	T
0.5370470000000012	0.0892040000000023	0.3746220000000022	T	T	T
0.7980489999999989	0.9132510000000025	0.7197060000000022	T	T	T
0.0060280000000006	0.2545920000000024	0.0572019999999966	T	T	T
0.0215910000000008	0.7832569999999990	0.0438789999999969	T	T	T
0.9090369999999979	0.0739969999999985	0.3665289999999999	T	T	T
0.3598619999999997	0.2468799999999973	0.0057460000000020	T	T	T
0.2543799999999976	0.5912050000000022	0.4081499999999991	T	T	T
0.4666840000000008	0.4926949999999977	0.7446120000000036	T	T	T
0.1185759999999974	0.9638580000000019	0.7345669999999984	T	T	T
0.6677630000000008	0.7909530000000018	0.0953939999999989	T	T	T
0.8161130000000014	0.2477549999999979	0.8500810000000030	T	T	T
0.9167679999999976	0.9278090000000034	0.5604870000000020	T	T	T
0.6877070000000032	0.5505610000000019	0.1997900000000001	T	T	T

0.3399069999999966 0.4872709999999998 0.9013279999999995 T T T

0.6306229999999999 0.0091499999999982 0.5979269999999985 T T T

0.3209370000000007 0.0168529999999976 0.8023579999999981 T T T

0.4792070000000024 0.7669390000000007 0.9104460000000003 T T T

0.7067059999999969 0.0209690000000009 0.2988479999999996 T T T

0.5810809999999975 0.3622060000000005 0.5380299999999991 T T T

0.1631330000000020 0.2180359999999979 0.9369090000000000 T T T

0.8548570000000026 0.2502199999999988 0.1843420000000009 T T T

0.5484020000000029 0.2708790000000008 0.1907139999999998 T T T

0.8856589999999969 0.6773450000000025 0.8073949999999996 T T T

0.3969949999999969 0.0288540000000026 0.5033249999999967 T T T

0.2114949999999993 0.7901060000000015 0.2510109999999983 T T T

0.1419410000000028 0.3605329999999967 0.2936049999999994 T T T

0.9767480000000006 0.9910679999999985 0.8882509999999968 T T T

0.3521909999999977 0.0676800000000028 0.1846129999999988 T T T

0.0138279999999966 0.5189329999999970 0.0505569999999977 T T T

0.5072919999999996 0.2432810000000032 0.8530850000000001 T T T

0.1108309999999975 0.1101499999999973 0.5406499999999994 T T T

0.3191630000000032 0.3757889999999975 0.5438469999999995 T T T

0.1515109999999993 0.7253189999999989 0.5659490000000034 T T T

0.8644990000000021 0.8197580000000002 0.1641750000000002 T T T

0.1727759999999989 0.7875980000000027 0.9167339999999982 T T T

0.6754230000000021 0.9700929999999985 0.9165240000000026 T T T

0.5203300000000013 0.7945270000000022 0.2480019999999996 T T T

0.8760150000000024 0.3126200000000026 0.5350350000000006 T T T

0.6608230000000006 0.5271010000000018 0.8844890000000021 T T T

0.0508740000000003 0.0467640000000031 0.2128340000000009 T T T

0.3668139999999980 0.5107380000000035 0.2167839999999970 T T T

0.4465530000000015 0.6756430000000009 0.5631649999999979 T T T

0.7084400000000031 0.6621310000000022 0.5571740000000034 T T T

#20% CaZrO$_x$ Ca$_2$Zr$_8$O$_{18}$

1.00000000000000

7.3410272353998645 0.0000000000000000 0.0000000000000000

1.9450438461546928 7.8932887814559836 0.0000000000000000

1.8538863021773251 1.3471291120958946 5.8944143367542186

Ca Zr O

2 8 18

Selective dynamics

Direct

0.1846430000000012 0.5512640000000033 0.6705309999999969 T T T

0.4764300000000006 0.1450930000000028 0.8953660000000028 T T T

0.9663109999999975 0.1661429999999982 0.9266569999999987 T T T

0.8631949999999975 0.9297579999999996 0.5019539999999978 T T T

0.2623630000000006 0.7714950000000016 0.0729100000000003 T T T

0.0896370000000033 0.3706419999999966 0.2506879999999967 T T T
0.5711709999999997 0.3258739999999989 0.3153179999999978 T T T
0.7978730000000027 0.7668490000000006 0.0643280000000033 T T T
0.6945669999999993 0.5307829999999996 0.6391040000000032 T T T
0.3987189999999998 0.9252180000000010 0.4925259999999980 T T T
0.8369119999999981 0.6870090000000033 0.7587660000000014 T T T
0.4280029999999968 0.6946080000000023 0.7697769999999977 T T T
0.0794580000000025 0.6190619999999996 0.0325849999999974 T T T
0.3417000000000030 0.1824539999999999 0.2888049999999964 T T T
0.7629189999999966 0.5105810000000019 0.2805129999999991 T T T
0.8980900000000034 0.1859460000000013 0.2853629999999967 T T T
0.8239870000000025 0.0098449999999985 0.8074719999999971 T T T
0.9748700000000028 0.3641799999999975 0.5989829999999969 T T T
0.5818409999999972 0.0775459999999981 0.5338250000000002 T T T
0.1625399999999999 0.3025760000000020 0.9395560000000032 T T T
0.3198500000000024 0.5141879999999972 0.2770119999999991 T T T
0.6900639999999996 0.7884320000000002 0.4165380000000027 T T T
0.4985580000000027 0.3939120000000003 0.6266729999999967 T T T
0.4925629999999970 0.8604079999999996 0.1168539999999965 T T T
0.1687480000000008 0.8361609999999970 0.4491030000000009 T T T
0.6861129999999989 0.3328369999999978 0.9669949999999972 T T T
0.2329319999999981 0.0024039999999985 0.7957040000000006 T T T
0.9711050000000014 0.9082140000000010 0.1493099999999998 T T T

#50% CaZrOx Ca$_4$Zr$_4$O$_{12}$

1.00000000000000

5.8091393580816542 0.0000000000000000 0.0000000000000000

-0.0004527840694200 5.5854471110591062 0.0000000000000000

-0.0000558416286114 0.0004313898720861 8.0298124100510861

Ca Zr O

4 4 12

Selective dynamics

Direct

0.5850000000000009 0.0537769999999966 0.1749719999999968 T T T
0.9651420000000002 0.5533190000000019 0.6754060000000024 T T T
0.4651100000000028 0.0962660000000000 0.6757449999999992 T T T
0.0842250000000035 0.5963210000000032 0.1759070000000023 T T T
0.5251230000000007 0.5749929999999992 0.9250809999999987 T T T
0.0253409999999974 0.0747929999999997 0.9251259999999988 T T T
0.5244080000000011 0.5751449999999991 0.4250430000000023 T T T
0.0246130000000022 0.0748800000000003 0.4252559999999974 T T T
0.9785949999999985 0.1931659999999980 0.1747670000000028 T T T
0.3241149999999990 0.8766010000000009 0.9861980000000017 T T T
0.2275240000000025 0.3759090000000000 0.8624089999999995 T T T

0.3223460000000031 0.8760059999999967 0.3625789999999967 T T T

0.4776140000000026 0.4568470000000033 0.1748499999999993 T T T

0.2258690000000030 0.3765619999999998 0.4866079999999968 T T T

0.7272350000000003 0.2739290000000025 0.8631540000000015 T T T

0.8235409999999987 0.7733619999999988 0.9871359999999996 T T T

0.8221509999999981 0.7744289999999978 0.3627480000000034 T T T

0.7261340000000018 0.2734439999999978 0.4865870000000001 T T T

0.0721419999999995 0.9563670000000002 0.6749420000000015 T T T

0.5725120000000032 0.6930669999999992 0.6748070000000013 T T T

#$ZrO_{1.69}$ $Zr_{13}O_{22}$

1.00000000000000

6.4139349676745274 0.0000000000000000 0.0000000000000000

2.9967134193335059 8.9413284007763565 0.0000000000000000

-2.4584451296606304 1.3343128033896583 7.5678505925647022

O Zn Zr H

22 0 13 0

Selective dynamics

Direct

0.4790810000000008 0.8500829999999979 0.5055240000000012 T T T

0.6533080000000027 0.7588580000000036 0.2114839999999987 T T T

0.3838500000000025 0.9995350000000016 0.9479200000000034 T T T

0.7460170000000019 0.4099199999999996 0.3487160000000031 T T T

0.6308530000000019 0.0919910000000002 0.7347960000000029 T T T

0.1689009999999982 0.8011679999999970 0.6880769999999998 T T T

0.5949919999999977 0.4743950000000012 0.6090360000000032 T T T

0.7179720000000032 0.7358180000000019 0.8806859999999972 T T T

0.8671500000000023 0.9422550000000030 0.1856780000000029 T T T

0.1987400000000008 0.6952250000000006 0.4022000000000006 T T T

0.2275589999999994 0.3666339999999977 0.5480639999999966 T T T

0.3395030000000006 0.6250069999999965 0.1463269999999994 T T T

0.9962549999999979 0.4929139999999990 0.1379370000000009 T T T

0.1827320000000014 0.0741000000000014 0.2280829999999980 T T T

0.7752710000000036 0.0058239999999969 0.4744129999999984 T T T

0.8843230000000020 0.6469280000000026 0.5881499999999988 T T T

0.5069220000000030 0.5529119999999992 0.9019369999999967 T T T

0.0948560000000001 0.1362409999999983 0.5435269999999974 T T T

0.1849080000000001 0.4305840000000032 0.8641500000000022 T T T

0.0336399999999983 0.8691979999999973 0.9458240000000018 T T T

0.9546029999999988 0.2352059999999980 0.8005560000000003 T T T

0.4277319999999989 0.2607909999999976 0.3046369999999996 T T T

0.8036329999999978 0.8536240000000035 0.6910030000000020 T T T

0.5094080000000005 0.3751779999999982 0.0923999999999978 T T T

0.5270289999999989 0.0459680000000020 0.2049980000000033 T T T

0.3090800000000016	0.2075609999999983	0.7850740000000016	T	T	T
0.9785690000000002	0.7179870000000008	0.1293179999999978	T	T	T
0.8623729999999981	0.1170380000000009	0.9933979999999991	T	T	T
0.8407529999999994	0.4516160000000013	0.8787519999999986	T	T	T
0.1155749999999998	0.9360939999999971	0.4356849999999994	T	T	T
0.2544940000000011	0.5523930000000021	0.6541210000000035	T	T	T
0.7308390000000031	0.2361030000000000	0.5304140000000004	T	T	T
0.5665770000000023	0.6408040000000028	0.4036740000000023	T	T	T
0.0731030000000032	0.2928739999999976	0.3081040000000002	T	T	T
0.3950889999999987	0.7747719999999987	0.9614199999999968	T	T	T

 # $H_2Zr_{18}O_{37}$

From lasp

1.00000000000000

6.3176553377543838	**0.0000000000000000**	**0.0000000000000000**
1.3193937393379493	**13.0322227591138589**	**0.0000000000000000**
-2.2247169391265982	**-0.5108037219212929**	**7.7643035678849852**

Na	**Zr**	**O**	**H**
0	**18**	**37**	**2**

Selective dynamics

Direct

0.6337350000000015	**0.8227279999999979**	**0.7374920000000031**	**T**	**T**	**T**
0.9032020000000003	**0.9848050000000015**	**0.1195769999999996**	**T**	**T**	**T**
0.3016659999999973	**0.0370559999999998**	**0.8959079999999986**	**T**	**T**	**T**
0.3903839999999974	**0.6620199999999983**	**0.3747260000000026**	**T**	**T**	**T**
0.7942859999999996	**0.7172479999999979**	**0.1552580000000034**	**T**	**T**	**T**
0.7396099999999990	**0.0819779999999994**	**0.7089780000000019**	**T**	**T**	**T**
0.1111459999999980	**0.5075130000000030**	**0.0019190000000009**	**T**	**T**	**T**
0.5207660000000018	**0.5578930000000000**	**0.7917849999999973**	**T**	**T**	**T**
0.1960270000000008	**0.1321060000000003**	**0.4706789999999970**	**T**	**T**	**T**
0.9559039999999968	**0.6104219999999998**	**0.5691479999999984**	**T**	**T**	**T**
0.0038780000000003	**0.2610450000000029**	**0.0161990000000003**	**T**	**T**	**T**
0.2561949999999982	**0.3960080000000019**	**0.4122759999999985**	**T**	**T**	**T**
0.0616389999999996	**0.8749729999999971**	**0.5319959999999995**	**T**	**T**	**T**
0.4416060000000002	**0.2992750000000015**	**0.8416799999999967**	**T**	**T**	**T**
0.6849020000000010	**0.4387129999999999**	**0.2345449999999971**	**T**	**T**	**T**
0.4926770000000005	**0.9258999999999986**	**0.3144020000000012**	**T**	**T**	**T**
0.2060699999999969	**0.7667160000000024**	**0.9553980000000024**	**T**	**T**	**T**
0.5624359999999982	**0.1924270000000021**	**0.2460659999999990**	**T**	**T**	**T**
0.1339690000000004	**0.3591189999999997**	**0.8898590000000013**	**T**	**T**	**T**
0.4840560000000025	**0.4609669999999966**	**0.9779109999999989**	**T**	**T**	**T**
0.9617050000000020	**0.4629759999999976**	**0.4518759999999986**	**T**	**T**	**T**
0.3248620000000031	**0.8966890000000021**	**0.7621869999999973**	**T**	**T**	**T**
0.9822350000000029	**0.4067349999999976**	**0.1500860000000017**	**T**	**T**	**T**

0.1249170000000035 0.2787980000000019 0.5818620000000010 T T T

0.5964880000000008 0.3365599999999986 0.3803180000000026 T T T

0.5326930000000019 0.1059500000000000 0.4507669999999990 T T T

0.1578230000000005 0.6700850000000003 0.1328389999999970 T T T

0.4100779999999986 0.1325780000000023 0.7286659999999969 T T T

0.7035509999999974 0.9241189999999975 0.5660489999999996 T T T

0.1687450000000013 0.6008020000000016 0.8218850000000018 T T T

0.8859420000000000 0.1244370000000004 0.2806619999999995 T T T

0.8055969999999988 0.5827439999999982 0.0075870000000009 T T T

0.3427920000000029 0.4938489999999973 0.2515980000000013 T T T

0.4924859999999995 0.7784079999999989 0.2003729999999990 T T T

0.3656119999999987 0.8120430000000027 0.4814229999999995 T T T

0.0043939999999978 0.7186200000000014 0.4043739999999971 T T T

0.8616790000000023 0.8121330000000029 0.9866940000000000 T T T

0.6857970000000009 0.2835189999999983 0.0842570000000009 T T T

0.6785080000000008 0.9833649999999992 0.8731000000000009 T T T

0.8299749999999975 0.8904500000000013 0.2868799999999965 T T T

0.5345999999999975 0.0290409999999994 0.1382919999999999 T T T

0.2985520000000008 0.5778109999999970 0.5431389999999965 T T T

0.4352629999999991 0.4039649999999995 0.6647140000000036 T T T

0.1986750000000015 0.9215570000000000 0.0527459999999991 T T T

0.9929630000000031 0.7840240000000023 0.7093899999999991 T T T

0.0006079999999997 0.0950229999999976 0.9614449999999977 T T T

0.3314370000000011 0.1967679999999987 0.0045939999999973 T T T

0.8159589999999994 0.4928299999999979 0.7243059999999986 T T T

0.6789739999999966 0.6013689999999983 0.3088770000000025 T T T

0.6604510000000019 0.6725339999999989 0.6219899999999967 T T T

0.1934389999999979 0.9822330000000008 0.3641059999999996 T T T

0.0352170000000029 0.0474379999999996 0.6336629999999985 T T T

0.4945280000000025 0.7180820000000026 0.8837710000000030 T T T

0.2272960000000026 0.2415239999999983 0.2904010000000028 T T T

0.7566240000000022 0.2417250000000024 0.7818159999999992 T T T

0.0047769999999971 0.3064540000000022 0.6305479999999974 T T T

0.7935909999999993 0.4265449999999973 0.6596070000000012 T T T

 # YZrO model Ov around Zr

From lasp

1.00000000000000

7.2233758623876181 0.0000000000000000 0.0000000000000000

0.0000008596965855 7.3398356513861112 0.0000000000000000

0.0000048929771778 -0.1913419756013136 10.3526544304033763

Zr O Y

14 31 2

Selective dynamics

Direct

0.2487220000000008	0.2482779999999991	0.2475450000000023	T	T	T
0.5000029999999995	0.9813410000000005	0.0091019999999986	T	T	T
0.7512850000000029	0.2482779999999991	0.2475450000000023	T	T	T
0.0000029999999995	0.4863879999999980	0.9986000000000033	T	T	T
0.2482990000000029	0.7461029999999980	0.2532739999999976	T	T	T
0.5000029999999995	0.5080969999999994	0.0123359999999977	T	T	T
0.7517089999999982	0.7461029999999980	0.2532730000000001	T	T	T
0.0000039999999970	0.0055819999999969	0.4901359999999997	T	T	T
0.2319140000000033	0.2588870000000014	0.7381960000000021	T	T	T
0.5000039999999970	0.0073909999999984	0.4973669999999970	T	T	T
0.7680930000000004	0.2588870000000014	0.7381960000000021	T	T	T
0.0000039999999970	0.5203020000000009	0.5028829999999971	T	T	T
0.2528440000000032	0.7759969999999967	0.7438999999999965	T	T	T
0.7471630000000005	0.7759969999999967	0.7438999999999965	T	T	T
0.0000039999999970	0.2625420000000034	0.1127779999999987	T	T	T
0.0000029999999995	0.2338090000000008	0.8529890000000009	T	T	T
0.2480159999999998	0.9925470000000018	0.1409319999999994	T	T	T
0.2606180000000009	0.0032730000000001	0.3880330000000001	T	T	T
0.5000020000000021	0.2396749999999983	0.0931289999999976	T	T	T
0.7519909999999967	0.9925489999999968	0.1409329999999969	T	T	T
0.7393890000000027	0.0032720000000026	0.3880339999999975	T	T	T
0.0000020000000021	0.7229510000000019	0.1155949999999990	T	T	T
0.0000029999999995	0.7381329999999977	0.8579790000000003	T	T	T
0.2659110000000027	0.4978139999999982	0.1457710000000034	T	T	T
0.2295719999999974	0.4999490000000009	0.3867550000000008	T	T	T
0.5000039999999970	0.7507859999999980	0.1198449999999980	T	T	T
0.5000029999999995	0.7259260000000012	0.8677059999999983	T	T	T
0.7340960000000010	0.4978130000000007	0.1457699999999988	T	T	T
0.7704349999999991	0.4999499999999983	0.3867540000000034	T	T	T
0.0000039999999970	0.2691609999999969	0.6043999999999983	T	T	T
0.0000039999999970	0.2247959999999978	0.3529029999999977	T	T	T
0.2269310000000004	0.0075519999999969	0.6316040000000029	T	T	T
0.2879659999999973	0.0202439999999982	0.8741679999999974	T	T	T
0.5000039999999970	0.2377600000000015	0.6386609999999990	T	T	T
0.5000039999999970	0.2556939999999983	0.3571680000000015	T	T	T
0.7730770000000007	0.0075519999999969	0.6316040000000029	T	T	T
0.7120400000000018	0.0202439999999982	0.8741679999999974	T	T	T
0.0000039999999970	0.7584000000000017	0.6098349999999968	T	T	T
0.0000039999999970	0.7700090000000017	0.3627380000000002	T	T	T
0.2496739999999988	0.5153809999999979	0.6497090000000014	T	T	T
0.2649079999999984	0.4434150000000017	0.9003129999999970	T	T	T
0.5000039999999970	0.7838629999999966	0.6214700000000022	T	T	T
0.5000029999999995	0.7483020000000025	0.3646039999999999	T	T	T

0.7503329999999977 0.5153809999999979 0.6497079999999968 T T T

0.7350989999999982 0.4434159999999991 0.9003129999999970 T T T

0.0000029999999995 0.9945099999999982 0.9996810000000025 T T T

0.5000039999999970 0.5055779999999999 0.5034009999999967 T T T

 # YZrO model Ov around Y

From lasp

1.00000000000000

7.3211058674366782 0.0000000000000000 0.0000000000000000

0.0000039795437113 7.2551813753889016 0.0000000000000000

0.0032430434314648 -0.0000031363253019 10.3304260760596627

Ca Zr O Y

0 14 31 2

Selective dynamics

Direct

0.2455730000000003 0.2512449999999973 0.2489180000000033 T T T

0.5023910000000029 0.9999979999999979 0.0096059999999980 T T T

0.7456940000000003 0.2496110000000016 0.2481369999999998 T T T

0.0063290000000009 0.4999979999999979 0.9926590000000033 T T T

0.2455730000000003 0.7487489999999966 0.2489160000000012 T T T

0.5038709999999966 0.4999979999999979 0.0038940000000025 T T T

0.7456940000000003 0.7503870000000035 0.2481379999999973 T T T

0.0074299999999994 0.9999979999999979 0.4976240000000018 T T T

0.2473000000000027 0.2321179999999998 0.7605459999999979 T T T

0.4987289999999973 0.9999979999999979 0.4961979999999997 T T T

0.7380629999999968 0.2531340000000029 0.7564899999999994 T T T

0.9906509999999997 0.4999970000000005 0.4859349999999978 T T T

0.2473010000000002 0.7678769999999986 0.7605459999999979 T T T

0.7380629999999968 0.7468620000000001 0.7564899999999994 T T T

0.9966000000000008 0.2771860000000004 0.1197540000000004 T T T

0.9925179999999969 0.2345869999999977 0.8586999999999989 T T T

0.2372000000000014 0.9999979999999979 0.1447959999999995 T T T

0.2590420000000009 0.9999990000000025 0.3905019999999979 T T T

0.4960889999999978 0.2390180000000015 0.1145160000000018 T T T

0.4997520000000009 0.2768269999999973 0.8663809999999970 T T T

0.7531269999999992 0.9999990000000025 0.1414230000000032 T T T

0.7388169999999974 0.9999940000000009 0.3926019999999966 T T T

0.9966000000000008 0.7228100000000026 0.1197549999999978 T T T

0.9925190000000015 0.7654080000000008 0.8586999999999989 T T T

0.2681820000000030 0.4999970000000005 0.1281930000000031 T T T

0.2330290000000019 0.4999960000000030 0.3809779999999989 T T T

0.4960900000000024 0.7609780000000015 0.1145160000000018 T T T

0.4997529999999983 0.7231669999999966 0.8663799999999995 T T T

0.7217690000000019 0.4999979999999979 0.1351820000000004 T T T

0.7595969999999994	0.4999990000000025	0.3728270000000009	T	T	T
0.0657739999999976	0.2951499999999996	0.6078680000000034	T	T	T
0.9948249999999987	0.2280599999999993	0.3632229999999979	T	T	T
0.2208979999999983	0.9999970000000005	0.6428549999999973	T	T	T
0.2708609999999965	0.9999990000000025	0.8867290000000025	T	T	T
0.4917200000000008	0.2336990000000014	0.6231059999999999	T	T	T
0.4979829999999978	0.2514099999999999	0.3583550000000031	T	T	T
0.7955040000000011	0.9999990000000025	0.6420040000000000	T	T	T
0.7153109999999998	0.9999979999999979	0.8801249999999996	T	T	T
0.0657750000000021	0.7048440000000014	0.6078680000000034	T	T	T
0.9948279999999983	0.7719340000000017	0.3632240000000024	T	T	T
0.2286390000000011	0.4999979999999979	0.8603230000000011	T	T	T
0.4917209999999983	0.7662970000000016	0.6231059999999999	T	T	T
0.4979810000000029	0.7485829999999964	0.3583550000000031	T	T	T
0.7522799999999989	0.4999979999999979	0.6360019999999977	T	T	T
0.7623829999999998	0.4999979999999979	0.8858680000000021	T	T	T
0.9920240000000007	0.9999990000000025	0.0040899999999979	T	T	T
0.5083109999999991	0.4999970000000005	0.4921229999999994	T	T	T